UNIVERSITÄTSKLINIKUM HAMBURG-EPPENDORF

Klinik und Poliklinik für Mund-, Kiefer- und Gesichtschirurgie

Direktor Prof. Dr. Dr. Heiland

Structural studies of *Pa*FabA- potential target for new antibiotics against *Pseudomonas aeruginosa*

Dissertation

zur Erlangung des Grades eines Doktors der Zahnmedizin
Der Medizinischen Fakultät der Universität Hamburg

vorgelegt von

Alessa Köhnke
aus Hamburg

Hamburg 2014

Angenommen von der Medizinischen Fakultät am: 07.07.2015

Veröffentlicht mit Genehmigung der Medizinischen Fakultät der Universität Hamburg.

Prüfungsausschuss, der/die Vorsitzende: Prof. Dr. Dr. Reinhard Friedrich

Prüfungsausschuss, zweite/r Gutachter/in: Prof. Dr. Wolfgang Hampe

Prüfungsausschuss, dritte/r Gutachter/in: Prof. Dr. Holger Rohde

Meinen Eltern

TABLE OF CONTENTS

LIST OF TABLES

LIST OF FIGURES

ABBREVIATIONS

∆GU	Gibbs free energy of unfolding
ACC	Acetyl-CoA carboxylase
ACP	Acyl carrier protein
al.	Alii
Å	Ångström
AMP	Adenosine monophosphate
APE	Alpha performance enhancer
Asp	Aspartic acid
ATP	Adenosine triphosphate
CoA	Coenzyme A
D	Aspartic Acid
DMSO	Dimethyl sulfoxide
DNA	Deoxyribonucleic acid
DTT	Dithiothreitol
e.g.	exempli gratia
E-coli (Ec)	*Echerichia coli*
EDTA	Ethylenediaminetetraacetic acid
ESBL	Extended-spectrum beta-lactamase
ESRF	European Synchrotron Radiation Facility
EU	European Union
FAB	Fatty acid biosynthesis
FAS	Fatty acid synthase
FEDESA	Fédération Européenne de la Santé Animale
g	gravity
Glu	Glutamic acid
H	Histidine
HAI	Healthcare-associated infection
His	Histidine
His6-tag	Hexa histidine-tag
HIV	Human immunodeficiency virus

ICU	Intensive care unit
IMAC	Immobilized metal affinity chromatography
IPTG	Isopropyl β-D-1-thiogalactopyranoside
K	Boltzmann-Konstante
LB	Lysogeny broth
MBC	Minimum bactericidal concentration
MES	2-(N-morpholino)ethanesulfonic acid
MIC	Minimum inhibitory concentration
N	Asparagine
NADPH	Nicotinamide adenine dinucleotide phosphate
NMR	Nuclear magnetic resonance
OD	Optical density
Pa	*Pseudomonas aeruginosa*
PDB	Protein Data Bank
psi	Pound-force per square inch
Q	Glutamine
RNA	Ribonucleic acid
rmsd	Root-mean-square deviation
rpm	Rotations per minute
RSV	Rous sarcoma virus
TEV	Tobacco Etch Virus
TLM	Thiolactomycin
Tm	Temperature of melting
TPB	Tryptone phosphate broth
UTI	Urinary tract infection
WT	Wild-type

1 INTRODUCTION

1.1 Medical relevance of developing new antibiotics

Antibiotics have been an essential part of modern medicine since their discovery in the early 20th century. Facilitating an efficient treatment of bacterial diseases, antibiotics have contributed to a significant decrease of mortality during the last 70 years (Wacha 1999).

Penicillin was discovered by the Scottish bacteriologist Alexander Fleming in 1928 (Fleming 1929). In the mid 1940s, penicillin was shown to be an efficient drug for the treatment of wound infections during the Second World War as well as against bacterial diseases such as syphilis and gonorrhea (Kardos and Demain 2011). In the United States, total cases of syphilis fell from 66 cases per 100,000 people in 1947 to 44 cases per 100,000 people in 1956 (Mahoney et al. 1943). Similar improvements were made in the treatment of tuberculosis using streptomycin. Total cases of tuberculosis in the United States decreased from 84,304 cases in 1953 to 22,436 in 1985 (Rieder et al. 1989).

The most common classes of antibiotics used today were discovered in the middle of the last century. The development of these drugs was generally focused on two strategies: discovery of compounds from natural sources, especially from fungi and the soil bacteria Actinomycetes, and the development of synthetic molecules (Kardos and Demain 2011). The main classes of antibiotics exploit a limited range of bacterial physiology: cell wall biosynthesis (β-lactams and glycopeptides), cell membranes (daptomycin, colistin), type II topoisomerases (fluoroquinolones), ribosomes (tetracyclines, aminoglycosides, macrolides, linezolid, streptogramins), transcription (rifampicin), and folate biosynthesis (sulphonamides, trimethoprim) (Fernandes 2006, Lange et al. 2007). Representing a relatively small set of chemical scaffolds, these classes of antibiotics have been modified over the past decades by synthetic tailoring. Only chemical groups in the periphery have been modified to upgrade

properties of the drug (Fischbach and Walsh 2009). Novel chemical scaffolds have greater potential to address the deficiencies of existing classes over further modification of existing antibiotics. However, there has been a decline in new approvals of antibiotics over the last 20 years and existing drugs are losing effectiveness more quickly than they can be replaced (Spellberg et al. 2004). On that score, it is obvious that this class of medical drugs, which has lead to an increase of life expectancy more than any other existing group of drugs, should be the subject of intensive research (Fischbach and Walsh 2009).

1.2 Bacterial resistance

The evolution of bacteria is tightly bound to fast responses to environmental changes ensuring the survival of the bacterial population. There is a time period of only a few years between introduction of an antibiotic for clinical use and the occurrence of resistant strains. Time for the emergence of resistance varies among organisms and antibiotics; for example, resistance against penicillin V was observed within one year but for vancomycin it was within 30 years (Walsh and Wright 2005).

Bacterial resistance mechanisms against antibiotics can be divided into several basic strategies: reduced accumulation of the drug associated with decreased permeability or increased efflux, modification or inactivation of the drug and target alteration (Figure 1) (Poole 2002). These mechanisms can be an intrinsic feature, result from mutation or the acquisition of exogenous resistance genes (Hogan and Kolter 2002, Normark and Normark 2002).

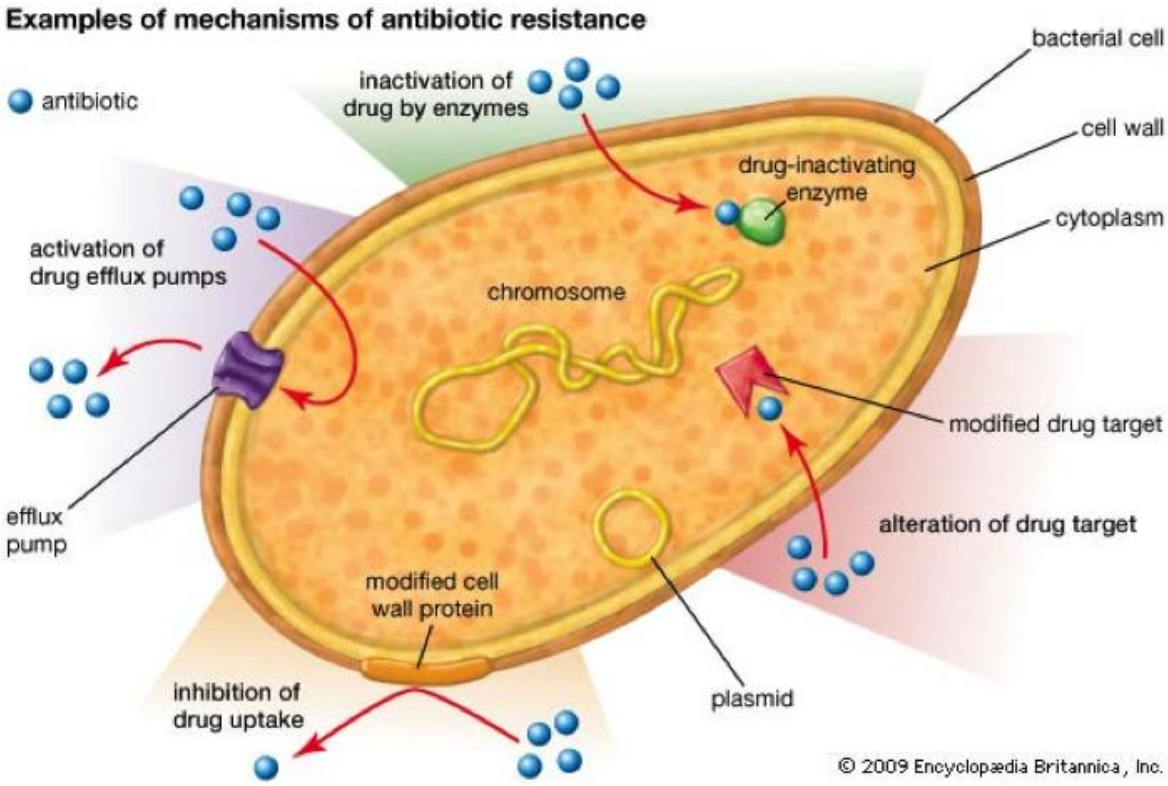

Figure 1: Examples of mechanisms of antibiotic resistance. Bacteria can develop resistance to antibiotics by multiple mechanisms: Inhibition of drug uptake due to modified cell wall, inactivation of the drug by drug-inactivating enzymes, alteration of the drug target or efflux pumps transport the compounds out of the cell (picture taken from Encyclopedia Britannica 2009).

Antibiotic resistance can be a result of mutations that alter the pre-existing genome of the cell (Avison 2005) or by acquisition of new genetic material from other bacteria in a process known as horizontal gene transfer. Three methods exist by which bacteria can transfer DNA from one cell to another: transformation, transduction or conjugation (shown in Figure 2). In transformation DNA is released on lysis of a cell and taken up by another cell. The antibiotic resistance gene can be integrated into the chromosome or the plasmid of the recipient cell. Generally, plasmids are circular DNA harbouring mainly accessory genes. They exist separately from the main bacterial chromosome and are replicated independently. Plasmids can contain genes that allow for the host to survive in potentially toxic environmental situations, such as the presence of antibiotics. Transduction occurs when phage-infected donor cells release bacteriophages containing host DNA, which is subsequently

transfered to recipient cells. During conjugation a mating bridge is formed between two cells and DNA is exchanged between them. Conjugation can transfer plasmids as well as other mobile genetic elements like transposons. They are sequences of DNA which carry their own recombinant enzymes that allow for transposition from one location to another (Furuya and Lowy 2006).

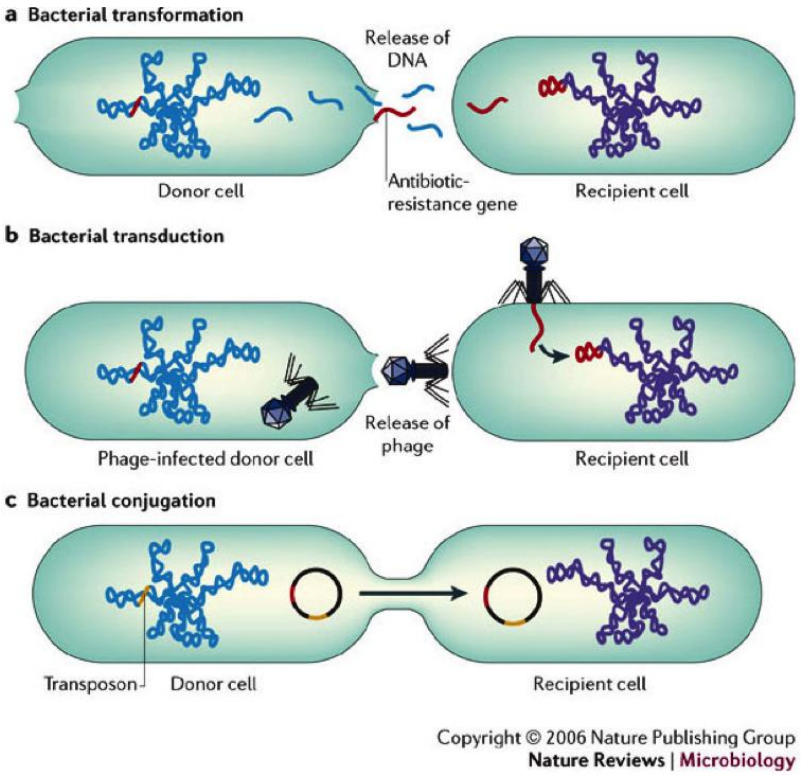

Figure 2: Mechanisms of horizontal gene transfer (antibiotic resistance gene shown in red). a) Transformation: DNA is released on lysis of an organism and is taken up by another organism. The chromosome or the plasmid of the recipient cell can integrate the antibiotic-resistant gene. b) Transduction: Transduction occurs when phage-infected donor cells release bacteriophages which transfer antibiotic-resistance genes to recipient cells. c) Conjugation: Direct contact between two cells facilitates that plasmids form a mating bridge across the cells and DNA is exchanged. It can result in the acquisition of antibiotic-resistance genes as well. Transposons are sequences of DNA which carry their own recombinant enzymes that allow for transposition from one location to another (Furuya and Lowy 2006).

The overuse of antibiotics and the inappropriate antibiotic treatments have been found to be important sources of risk for reaching antibiotic resistance. In

industrialized countries misuse or overuse mostly result from incorrect prescription or administration of antibiotics (Fischbach and Walsh 2009).
In recent years, many household products for cleaning and disinfection within the home environment containing antibacterial agents have reached the market. It was thought that most cleaning and hygiene products use multiple targets for degrading and inhibiting bacteria. Products containing alcohol have been used for decades without any concerns of resistance, because they are non-specific (White and McDermott 2001). Concern over the use of products containing triclosan (2,4,4'-trichloro-2'-hydroxyphenyl ether) has been raised, since research has shown that triclosan involves next to non-specific mechanisms a special enzyme of fatty acid synthesis as well (McMurry et al. 1998).
Apart from human medicine, antibiotics were used in veterinary medicine and animal husbandry. The European Federation of Animal Health (FEDESA) suggested that in the EU annually 50 % of all antibacterial drugs are given to animals (FEDESA 1998). These antibiotics are not only used for prevention and treatment of infections, they are continuously added to animal feeds as “performance enhancers” (APEs) to promote growth, increase feed efficiency and decrease waste production. Therefore, the general handling of antibiotics themselves has to change to delay the evolution of new resistant strains.

1.3 Healthcare-associated infections

Intensive Care Units (ICUs) in particular are faced with the fast occurrence and spread of resistant strains. Healthcare-associated infections (HAIs), also known as nosocomial infections, are infections acquired by patients during the course of receiving treatment in a hospital or healthcare service unit. In the United States annual direct hospital costs for HAIs are estimated to be $ 4.5 billion (Martone et al. 1992). The Centre For Disease Control and Prevention (CDC) estimated that approximately 1.7 million HAIs emerged in U.S. hospitals in 2002 and approximately 98,987 deaths were associated with HAIs (Klevens et al. 2007).

The high frequency of drug resistance emerges because of the crowding of people with high levels of disease within a small area. Environmental cleaning and optimal hand hygiene behaviour are essential measures to prevent the spread of resistant pathogens (Rampling et al. 2001, Pittet et al 2006), but economic pressures often cause reductions in nursing staff and cleaning personnel. This situation enhances the probability of person-to-person transmission of these microorganisms (Carlet et al. 2004, Haley and Bregman 1982, Kollef and Fraser 2001).

In addition to standard infection control techniques, several prevention strategies are applied to delay the occurrence of antibiotic resistance (Kollef and Micek 2005). One of these methods is the use of combination therapy (using two antibiotics simultaneously) and sequential therapy (switching two antibiotics). It was shown that sequential therapy can slow down the evolution of resistance when antibiotics are used in a specific order (Perron et al. 2012). Another method is the periodic rotation of two or more antibiotics within a hospital. However, clinical trials testing these methods against different bacterial infections led to mixed results (Bal et al. 2010, Bennett et al 2007, Reinhardt et al. 2007, Sandiumenge et al. 2006, Warren et al. 2004). Finally, the application of antibiotic guidelines or protocols has been implemented to avoid unnecessary antibiotic treatments and increase the effectiveness of the prescribed drug. To improve antibiotic efficiency the drug dosing, interval of administration and duration of treatment should be optimized (Kollef and Fraser 2001).

1.4 Pseudomonas aeruginosa

Next to *Staphylococcus aureus* (*MRSA*), *Enterococcus faecium, Streptococcus pneumoniae Acinetobacter baumannii, Klebsiella pneumonia* and *Escherichia coli*, *Pseudomonas aeruginosa* is one of the main pathogens showing worrisome resistance rates (Lister et al. 2009).

Generally only a small number of bacterial species are able to cause disease in individuals with normal host defenses (pathogenic bacteria). However,

opportunistic bacteria, which are generally not pathological but can cause disease in immunocompromised or elderly people. The normal microflora predominantly consists of commensal bacteria, though some commensals can be opportunistic bacteria as well. *Pseudomonas aeruginosa* is one of these opportunistic pathogens. It is a rod-shaped, Gram-negative, none-spore forming bacterium with polar flagella and belongs to the class of Gammaproteobacteria. They are viable aerobes in water and soil and can infect animals, plants or humans (Filiatrault et al. 2006, Lewenza et al. 2005, Stover et al. 2000).

P. aeruginosa has several virulence mechanisms: pili and other adhesins seem to be relevant for colonization on mucosa membranes and other surfaces (Ramphal and Pier 1985, Doig et al. 1988, Prince 1992). For the formation of biofilms *P.aeruginosa* produces a mucoid exopolysaccharide matrix (Hoiby et al. 2001). Biofilms are complex, organized communities of microorganisms growing on biotic and abiotic surfaces (Wimpenny 2000). Bacteria undergo significant changes during their transition from planktonic organisms to cells that are part of a complex, surface-attached community, in which the bacteria are protected from the host innate and immune defenses and are up to 1000 times less susceptible to antibiotics (Costerton et al. 1999, Klemm et al. 2007). Several nosocomial infections are linked to the formation of biofilms on the surfaces of medical devices such as central venous or urinary catheters, cardiac valves (Donlan et al. 2002, Stewart et al. 2001), and orthopedic devices (Gristina et al. 1994).

P. aeruginosa produces and secretes several substances, including elastase, alkaline protease, cytotoxin, phospholipase C and rhamnolipid, that seem to be important for tissue damage and invasion (Berka and Vasil 1982, Kharami et al. 1989, Lutz et al. 1991, Read et al. 1992, Komori et al. 2001). The release of endotoxin and the production of exotoxin A and exoenzyme S are related to the local and systemic toxicity of *P. aeruginosa* (Pollack 1980, Nicas 1985). A quorum-sensing regulatory mechanism controls the production of exoenzymes and other virulence factors by coordinating expression of the corresponding genes to when cell densities exceed certain values. Therefore this mechanism ensures that virulence factors are only produced when there is a chance that

the infection will overcome the host defenses and it reduces the possibility of immunization against these products (Van Delden 1998).

1.4.1 Clinical relevance of *P. aeruginosa*

Data from the CDC and the National Nosocomial Infection Surveillance System from 1986-1998 show that *P. aeruginosa* was identified as the fifth most frequently isolated nosocomial pathogen, accounting for 9 % of all HAIs. It is the second most common cause of nosocomial pneumonia (17 %), the third most common cause of urinary tract infections (UTIs) (7 %), the fourth most frequently isolated bacterium in surgical site infections (8 %) and the seventh most common isolated pathogen in bloodstream infections (2 %) (Emori and Gaynes 1993, National Nosocomial Infections Surveillance System 1998). In Europe, *P. aeruginosa* was the second most common cause of infections in ICUs, causing 30 % of pneumonias, 19 % of UTIs and 10 % of bloodstream infections (Spencer 1996). In hospitals *P. aeruginosa* can be isolated from various sites, in particular water-related sites, or places where moisture or humidity is high, for example taps, sinks, soap, showers, mops, antiseptics and medicines. It was also found on respiratory therapy equipment and physiotherapy or hydrotherapy pools (Pollack 2000). Outside of hospitals, *P. aeruginosa* has been identified in swimming pools, whirlpools, hot tubs, contact lens solution, home humidifiers, soil samples and vegetables (Pollack 2000, Pitt 1998, Harris et al. 1984). Colonization rates of *P. aeruginosa* on human body sites are 0-2 % for skin, 0-3.3 % for the nasal mucosa, 0-6.6 % for the throat and 2.6-24 % for fecal samples (Morrison and Wenzel 1984).

The most frequent community-acquired infections caused by *P. aeruginosa* are infections of the ear canal, folliculitis after bathing in contaminated water and cheratitis as a result of contaminated contact lenses (Bottone and Perez 1993, Pollack 2000, Holland et al. 1993). Other infections by the pathogen can lead to malignant otitis externa of underlying tissues and sometimes of the temporal bone and basilar skull, osteomyelitis of the calcaneus in children and

endocarditis in intravenous drug users due to the injection of contaminated drug solutions (Rubin and Yu 1988, Fisher et al. 1985, Rajashekaraiah et al. 1981).
For certain subgroups of patients, particularly mechanically ventilated patients, *P. aeruginosa* is the most frequent cause for nosocomial pneumonia (Mayhall 1997). Invasive procedures like catheterization increase the probability of developing a nosocomial UTI. UTIs and wound infections, especially in burn patients, can be complicated by bacteremia (Pollack 2000, Mousa 1997). In addition there is a higher risk for developing a bacteremia caused by *P. aeruginosa* in all situations associated with neutropenia and mucosal ulcerations, like cancer chemotherapy, organ transplantation or hematological malignancies (Pollack 2000, Koll and Brown 1993, Aquino et al. 1995, Fishman and Rubin 1998, Pizzo 1999). Diabetes mellitus, immunoglobulin deficiency states, steroid therapy, burns and surgery are other predisposing factors (Pollack 2000). *P. aeruginosa* is the most frequent detected bacteria in the lungs of cystic fibrosis patients (Pollack 2000, Davies 2002). Chronic infection by *P. aeruginosa* is the predominant cause of mortality in people with cystic fibrosis despite the use of antibiotics (Murray et al. 2007). In most patients chronic colonization induces progressive lung damage, and in some cases it leads to respiratory failure and death (Burns et al. 1993, Hoiby 1993, Welsh et al. 1995).

1.4.2 Resistance of *P. aeruginosa* against antibiotics

Table 1: The main mechanisms of resistance to antibiotics employed by *P. aeruginosa* (adapted from Dalhoff et al. 2006, Poole 2004, Rossolini and Mantengoli 2005).

	Resistance mechanisms					
	Inhibition of drug uptake	Efflux pumps	Inactivation by enzymes		Alteration of drug target	
Antibiotics			β-Lactamase	Aminoglycoside modifying enzymes	Mutations in topoisomerase	Ribosomal methylation
β-Lactams						
Penicillins		✓	✓			
Cephalosporins		✓	✓			
Aztreonam						
Carbapenems	✓		✓			
Imipenem	(✓)	✓	✓			
Meropenem						
Aminoglycosides						
Amikacin		✓		✓		✓
Gentamycin		✓		✓		✓
Netilmicin		✓		✓		✓
Tobramycin		✓		✓		✓
Fluoroquinolones		✓			✓	

During antimicrobial chemotherapy against *P. aeruginosa*, resistance can result in therapeutic failures. It is usually linked with higher morbidity and mortality, increased hospital stay and costs (Carmeli et al. 1999). *P. aeruginosa* displays intrinsic resistance to a variety of commonly used antimicrobial agents due to three major factors: the low permeability of the outer membrane, the production of antibiotic-inactivating enzymes and the constitutive expression of several multidrug efflux-pumps (Hancock 1998). These three main resistance mechanisms have been observed in clinical isolates of the three main classes of current antipseudomonal agents (β-lactams, fluoroquinolones and aminoglycosides) (McGowan 2006, Thomson and Bonomo 2005).

Outer membrane porin channels limit the access of hydrophilic antibiotics, such as carbapenems, to the periplasmic space. Consequently, the appearing imipenem resistance of *P. aeruginosa* during therapy is associated with the alteration of the OprD porin to reduce the influx of imipenem (Dalhoff et al. 2006).

The most important efflux systems involved in *P. aeruginosa* resistance belong to the Hydrophobic/Amphiphilic Efflux 1 family. Generally, efflux systems are responsible for extrusion of toxic substances and antibiotics outside the cell. Some of them, such as MexAB-OprM, are expressed at low levels in wild-type strains and confer intrinsic resistance to penicillins, cephalosporins, aztreonam, meropenem and fluoroquinolones. Other efflux systems are significantly induced in response to antibiotic pressure and are only expressed in low levels in the absence of antibiotics, such as MexXY-OprM. Some efflux systems are only expressed in the presence of antibiotics (MexCD-OprJ and MexEF-OprN) (Poole and Srikumar 2001).

Expressed enzymes can inactivate β-lactams and aminoglycosides. While inactivation of β-lactams occurs through hydrolysis of the β-lactam ring aminoglycosides are inactivated through chemical modification of the antibiotic (e.g. acetylation, adenylation and phosphorylation). Extended-spectrum β-lactamases (ESBLs) confer resistance to all β-lactams, except carbapenems (Weldhagen et al. 2003). The metallo-β-lactamase is able to inactivate all subclasses of β-lactams, except monobactams (Walsh et al. 2005). These enzymes have been found in a limited number of geographical areas (Weldhagen et al. 2003). Enzymes inactivating aminoglycosides were found in up to 20 % in clinical isolates in Europe and Latin America (Poole 2005).

P. aeruginosa is able to acquire resistance to many of the antipseudomonal agents. A common example is emerging resistance to new antipseudomonal β-lactams resulting from mutations in β-lactamases. Other mutations can lead to changes in expression levels of resistance-associated proteins such as increased production of AmpC β-lactamase (Livermore 1995), decreased expression of the OprD porin (Livermore 2001) and the up-regulation of efflux systems (Kohler et al. 1997). Another possibility is the acquisition of secondary β-lactamase genes by horizontal gene transfer (Livermore 1995). Aminoglycoside-modifying enzymes encoded by horizontally acquired resistance determinants or mutations reducing aminoglycoside accumulation in the cell can induce resistance to aminoglycosides (Hancock 1998). Mutations causing lipopolysaccharide changes or up-regulation of efflux systems can be

responsible for decreased accumulation of aminoglycosides (Bryan et al. 1984, Jo et al. 2003). Resistance to fluoroquinolones can be acquired from mutations causing the up-regulation of efflux systems (Poole 2001) or mutations of the topoisomerase target (Akasaka et al. 2001). Both mutations can induce cross-resistance to all fluoroquinolones (Piddock 1999). An increasing resistance level to certain antibiotics can arise when different mechanisms cooperate. The level of resistance to meropenem can increase when the loss of OprD and up-regulation of the MexAB-OprM efflux system act in combination, for example (Kohler and Pechere 2001). Contrastingly, the level of resistance to imipenem is increasing if the loss of OprD and high-level production of AmpC cooperate (Livermore 1992).

1.5 Remaining treatment options

As a consequence of antibiotic resistance, there are a limited number of antibiotics left that can be used against infections caused by *P. aeruginosa*. Some antibiotics used in current treatments are the penicillin derivative piperacillin, third generation cephalosporins such as ceftazidime, the monobactam aztreonam, fluoroquinolones, carbapenems such as like imipenem and meropenem, and some aminoglycosides such as gentamycin, tobramycin, netilmycin and amikacin (Giamarellou and Kanellakopoulou 2008, Rahal 2008). Due to their neurotoxicity and nephrotoxicity polymyxins, including polymyxin B and polymyxin E (colistin) are only in use against multidrug-resistant strains. These antibiotics are rarely used for typical bacterial infections due to their side effects, but they have recently been relaunched for use in tackling life-threatening infections as a last resort treatment (Yuan and Tam 2008).

Depending on severity of the disease, current treatment guidelines recommend a combination chemotherapy regimen. Typically, a member of the β-lactam class should be administered with an aminoglycoside or a fluoroquinolone (Bassetti et al. 2008). Combination chemotherapy with at least two different antibiotics is recommended for infections such as endocarditis, nosocomial pneumonia and bacteremia (Pollack 2000). Since synergism between

aminoglycosides and β-lactams has been observed *in vitro*, this combination remains the favored option (Giamarellou et al. 1984, Burgess and Hastings 2000). Early aggressive combination chemotherapy is recommended for initial colonization episodes in cystic fibrosis patients and the aim of this strategy is to avoid a chronic infection as long as possible (Doring et al. 2000). For the treatment of infections caused by multidrug-resistant *P. aeruginosa*, *in vitro* susceptibility data are important, due to the frequency and variability of acquired resistance. Testing of the susceptibility is well standardized for most anti-pseudomonal drugs, except for polymyxin B and E (Kiska and Gilligan 2003). For the polymyxins, minimum inhibitory concentration (MIC) or minimum bactericidal concentration (MBC) determination is recommended because the correlation with disk diffusion testing is relatively poor (Gales et al. 2001b). However, empirical regimens should be started before getting the results from susceptibility testing and cultures, in cases where this bacterium is suspected and the infection seems to be lethal. The choice of antibiotics requires different considerations. A number of factors should be considered including the nature and source of the infection, information concerning the epidemiology of resistance phenotypes in the individual setting, pharmacokinetic parameters, underlying risk factors and diseases, and hospital prescription policy (Pollack 2000).

Data from the SENTRY Antimicrobial Surveillance Program comparing clinical isolates from Europe, North America, Latin America and the Asia-Pacific region from 1997-2000 show that amikacin, piperacillin-tazobactam and carbapenems are the most efficient antibiotics against *P. aeruginosa* worldwide while ticarcillin and aztreonam show the lowest activities (Jones et al. 2002). Susceptibility rates show geographical differences. In general the lowest susceptibility rates were determined in Latin America and the highest rates in North America and in the Asia-Pacific region. But this general pattern is not transferable for all antibiotics: fluoroquinolones are more active in the Asia-Pacific region than in North America and for aztreonam, a higher rate was observed in Europe than in the other areas (Jones et al. 2002). Apart from geographical differences, diversity within a single hospital has been observed. For some β-lactams, such

as carbapenems, ceftazidime and ticarcillin-clavulanate, susceptibility rates in the United States from 1998-2001 were lower in ICUs than in general wards (Karlowski et al. 2003). Other data from ICU isolates show that there are generally higher resistance rates in Europe than in America (Karlowski et al. 2003, Hanberger et al. 2001). In the SENTRY program, multidrug-resistance is defined as resistance against piperacillin, ceftazidime, imipenem and gentamycin. Rates are higher in Latin America (8 %), lower in Europe (5 %) and less than 2 % in North America and the Asia-Pacific region (Gales et al. 2001a). Nevertheless one of the most threatening development is the emergence of strains that are resistant to all available anti-pseudomonal drugs, reminiscent of conditions typical for the pre-antibiotic era. This development highlights the importance of the search for new anti-pseudomonal antibiotics with alternative mechanisms of action (Giamarellou 2002).

In recent years, only one new anti-pseudomonal drug (the carbapenem, doripenem) has reached the market. No other introduced Gram-negative drug covers *P. aeruginosa* in their spectrum (Poulakou and Giamarellou 2008). As a consequence, there is a significant interest in generating new antibiotics with new targets in *P. aeruginosa*. Enzymes involved in fatty acid biosynthesis remain interesting as targets because of the different enzymes that carry out fatty acid synthesis in bacteria and humans. This offers the prospect of inhibitors with different host and target specificity.

1.6 Fatty acids

Fatty acids are essential components of all living organisms, having four major physiological roles. They are an important source of energy in the cell and are stored as triacylglycerol through an ester linkage to glycerol. Fatty acids detached from triacylglycerols are oxidized to power the cell or the organism. Fatty acids are important components of biological membranes by forming the building blocks for phospholipids and glycolipids. Moreover they can modify many proteins by their covalent attachment and fatty acid derivatives serve as intracellular messengers and hormones (Lehninger et al. 1998).

Fatty acids are carboxylic acids with long hydrocarbon chains. The chain length generally varies from 4 to 36 carbons. The chain is non-polar and an important counter balance to the polar acid functional group. Unsaturated fatty acids contain one or more double bonds between the carbons. Saturated fatty acids have all bonding positions occupied by hydrogen (Lehninger et al. 1998).

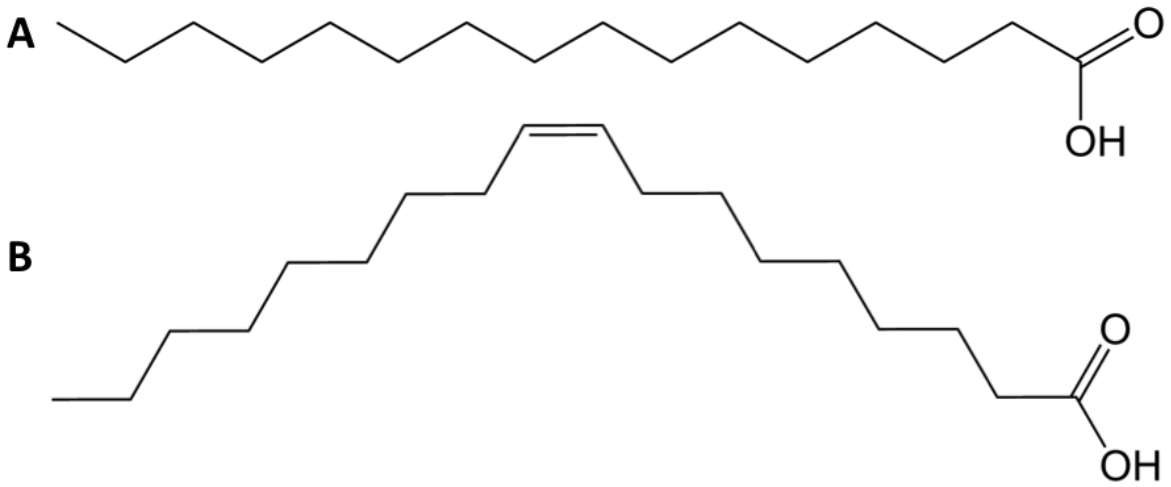

Figure 3: Fatty acids consisting of a hydrocarbon chain and a carboxylic acid group. a) Palmitic acid b) Oleic acid

Before they participate in metabolism fatty acids are activated through the formation of a thioester linkage to coenzyme A. Adenosine triphosphate (ATP) drives the formation of the thioester linkage between the carboxyl group of the fatty acid and the sulfhydryl group of coenzyme A. This activation reaction is catalyzed by acyl CoA synthetase (Lehninger et al. 1998).

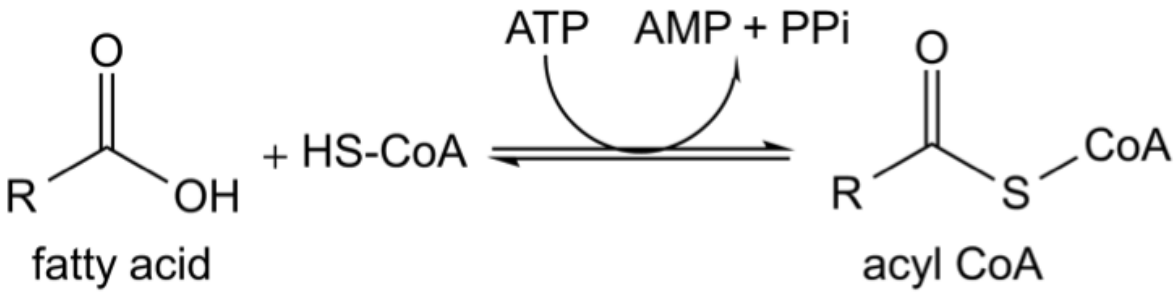

Figure 4: Activation of a fatty acid through the linkage to coenzyme A.

Generally two related, but distinct, biosynthetic systems can synthesize fatty acids. The type II fatty acid synthase (FAS II) is found in plants, bacteria and other microorganisms, and is especially involved in membrane formation. This synthesis is carried out by a series of discrete enzymes (Cronan 2003, White et al. 2005). Type I fatty acid synthase (FAS I) is located in the mammalian cytosol and in fungi. In humans, the synthesis of fatty acids primarily takes place in the cytoplasm of adipose and liver tissue as well as in the central nervous system and lactating mammary gland (Lehninger et al. 1998). The multifunctional polypeptide contains all of the enzymatic domains required for fatty acid biosynthesis. The active form of this protein is a dimer (Lehninger et al. 1998). Although the reactions catalyzed by FAS I and II are the same, there are important structural differences in the enzymes (Heath and Rock 2004).

In both fatty acid elongation cycles, the hydrophobic chain is extended by two carbons in each round. Prior to chain elongation malonyl-CoA must be produced by acetyl-CoA carboxylase (ACC) in a separate reaction (Figure 5).

The acyl moiety is carried by a flexible phosphopantetheine group attached to the acyl carrier protein (ACP) domain. In the end the palmitic acid is released from the complex by the thioesterase domain (Lehninger et al. 1998).

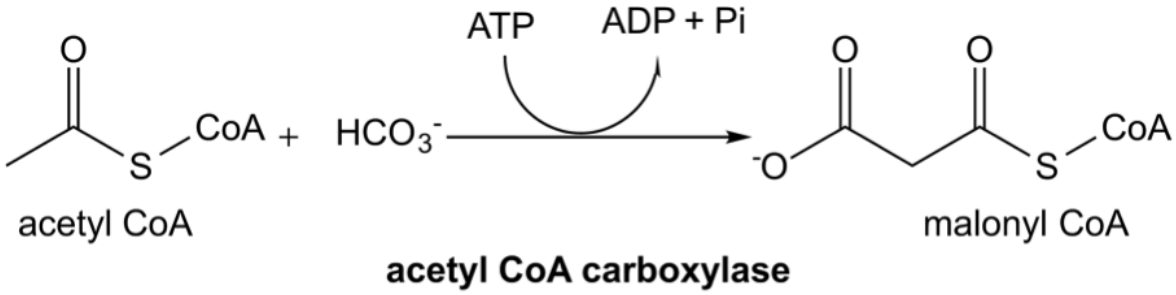

Figure 5: Formation of malonyl CoA, catalyzed by acetyl CoA carboxylase, is the committed reaction in fatty acid synthesis.

The elongation cycle consists of the enzymatic steps of decarboxylative condensation, reduction, dehydration and another reduction, as shown in Figure 6. The major product of fatty acid biosynthesis is palmitic acid (C16). This synthesis requires a series of 37 sequential reactions from acetyl-CoA and

malonyl-CoA. NADPH is the electron donor in reductive reactions. Without being released from the complex, the intermediates are shuttled from one catalytic site to another.

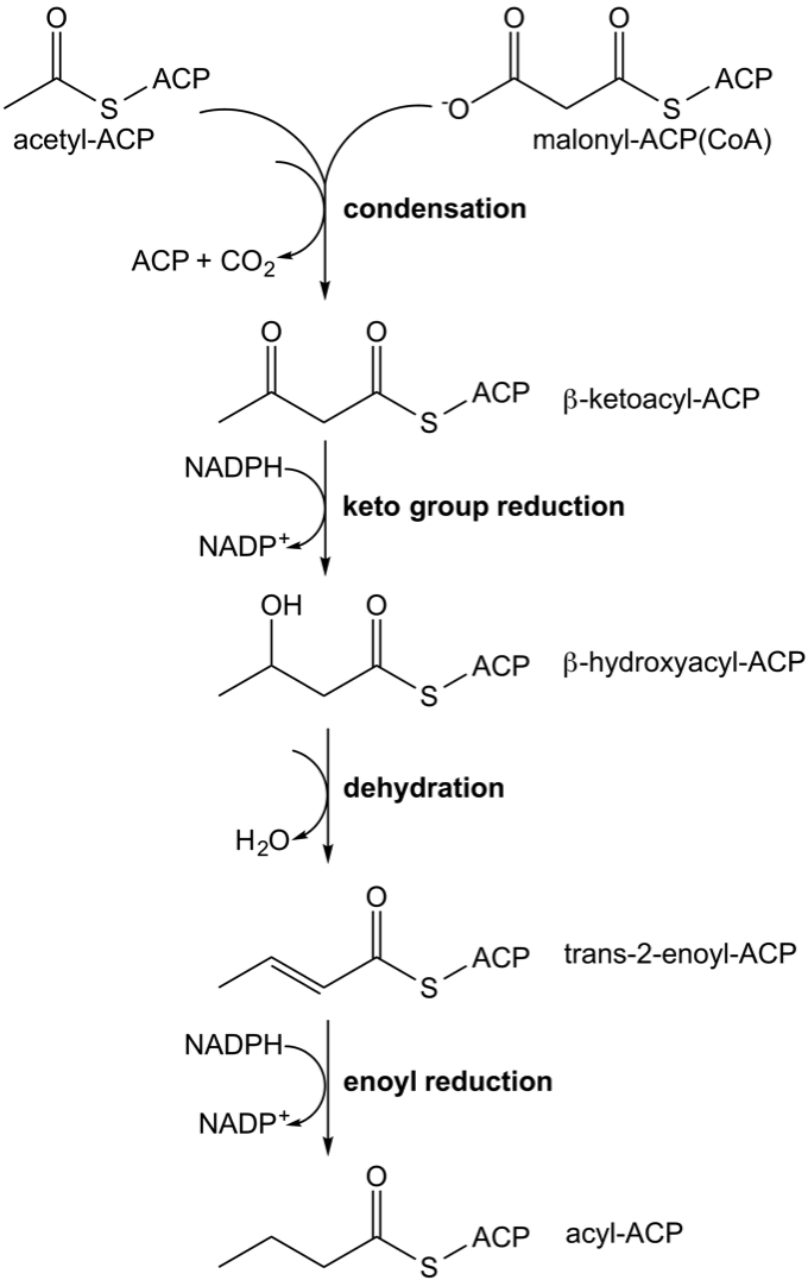

Figure 6: Fatty acid synthesis. Fatty acids are synthesized by the repetition of four reactions: condensation, reduction, dehydration and reduction.

The reaction sequence of the type II pathway is carried out by different soluble proteins, which are all encoded by separate genes. Many of them have been

identified and characterized in *E. coli* (White et al. 2005). Enzymes of FAS II seem not to be physically associated, although transient interactions are thought to take place (Honeyman and Fawcett 2000). The intermediates are shuttled between the enzymes by means of an ACP (Magnuson et al. 1993, Rock and Cronan 1996). The cycle is, as with FAS I, composed of four steps. In some cases, multiple enzymes are available to catalyze a single step. These enzymes are suggested to have different substrate specificities and physiological functions.

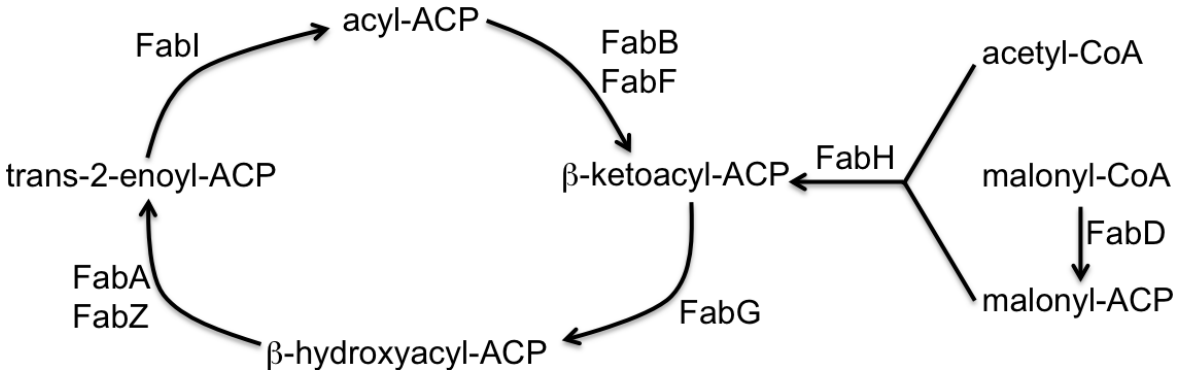

Figure 7: Enzymes of fatty acid elongation in *E. coli* (Heath and Rock 1996). The production of fatty acids in bacteria is catalyzed by a series of proteins encoded by separate genes that carry out the individual enzymatic steps. See table 2 for the activities of the enzymes involved in fatty acid elongation.

Table 2: Function of enzymes involved in fatty acid elongation

Protein	Enzyme activity
FabA	β-hydroxyacyl-ACP dehydratase/isomerase
FabB	β -ketoacyl-ACP synthase I
FabD	Malonyl CoA:ACP transacylase
FabF	β -ketoacyl-ACP synthase II
FabG	β -ketoacyl-ACP reductase
FabH	β -ketoacyl-ACP synthase III
FabI	Trans-2-Enoyl-ACP reductase I
FabZ	β -ketoacyl-ACP dehydratase

Malonyl-ACP generation is catalyzed by ACP transacylase, the enzyme known as FabD in *E. coli* (Harder et al. 1974). The first cycle of FAS starts with the condensation of malonyl-ACP with acetyl-CoA; this initiation step is catalyzed by the β-ketoacyl-ACP synthase III (FabH) (Jackowski and Rock 1987, Tsay et al. 1992, Heath et al. 2001). The other β-ketoacyl-ACP synthases (I and II) are known as FabB and FabF. Both enzymes operate in subsequent cycles of FAS (D`Agnolo et al. 1975 a and b, Garwin et al. 1980, Rock and Cronan 1996). In the second step, the keto group of the substrate acyl chain is reduced to a hydroxyl group by the NADPH-dependent FabG (β-ketoacyl-ACP reductase) (Rock and Cronan 1996). The β-hydroxyacyl-ACP dehydratases FabA and FabZ participate in the third step of the elongation cycle. They catalyze the conversion of β-hydroxyacyl-ACP to trans-2-acyl-ACP, where the hydroxyl group is removed from position three of the fatty acyl hydrocarbon chain. In the fourth step, trans-2-enoyl-ACP is reduced to acyl-ACP by the NAD(P)H-dependent FabI (trans-2-enoyl-ACP reductase) (Rock and Cronan 1996). The resulting acyl-ACP is two carbons longer. It can re-enter the cycle for elongation again or if it is 16-18 carbons in length, it can be transferred to glycerol phosphate to produce phospholipids (Rock and Cronan 1996).

FabA and FabB participate in the synthesis of unsaturated fatty acids. In addition to dehydration, FabA carries out the isomerization of trans-2- decenoyl-ACP to cis-3-decenoyl-ACP, which is an essential step in the biosynthesis of unsaturated fatty acids as it controls the divergence of the metabolic pathways of saturated and unsaturated fatty acid synthesis (Heath and Rock 1996). FabB elongates this unsaturated fatty acid that branches off the FAS II pathway (Clark et al. 1983). For *E. coli*, the crystal structures of the enzymes belonging to the elongation cycle have been determined: FabB (Price et al. 2001), FabF (Huang et al. 1998; Price et al. 2003), FabG (Price et al. 2001), FabA (Leesong et al. 1996) and FabI (Baldock et al. 1998).

Inhibition of enzymes of fatty acid synthesis has been reported: ACC is a target for widely used commercial herbicides in plants (Nikolskaya et al. 1999). The broad-spectrum pyrrolidinedione antibiotics, such as moiramide B, also target ACC (Freiberg et al. 2004). A FabD inhibitor, called corytuberine, has been

identified, though it is still unclear if its antibacterial activity can be attributed to its ability to inhibit FabD (Liu et al. 2006). FabH is also an interesting target for drug discovery. Development of compounds acting against FabH in *Staphylococcus aureus* was successful, but these inhibitors were less effective against FabH homologs from *E. coli* and *Haemophilus influenza* (Khandekar et al. 2001). Cerulenin was the first discovered inhibitor for FabB and FabF (Kauppinen et al. 1988) and has since been joined by thiolactomycin (TLM) (Hayashi et al. 1984). TLM has only modest antibacterial activity (Noto et al. 1982), but possesses favorable physical properties (Miyakawa et al. 1982) and a broad-spectrum activity against pathogens like *M. tuberculosis* (Slayden et al. 1996) and malaria (Jones et al. 2004). Platensimycin and platensin target FabB and FabF as well (Wang et al. 2006, Wang et al. 2007). FabI is the most explored target, after the discovery of isoniazid for the treatment of tuberculosis (Banerjee et al. 1994) and the antibacterial agent triclosan (Levy et al. 1999, Heath et al. 1998). The problem of these FabI inhibitors is that organisms containing FabK, such as *Streptococcus pneumonia*, are resistant to these drugs. FabK shows no sequence similarity to FabI, but catalyzes the same reaction (Marrakchi et al. 2003). There is only one compound reported to inhibit FabG (Epigallocatechin gallate), but this polyphenol have multiple targets in the cell, thus it is not a specific FabG inhibitor (Zhang and Rock 2004). Two compounds have been described to target FabZ in *Plasmodium falciparum* (Sharma et al. 2003). In spite of intensive research, at this point of time, the only enzyme inhibited by antibiotics in clinical use is still FabI.

1.7 FabA

Apart from dehydration, FabA carries out the isomerization of trans-2- to cis-3-decenoyl-ACP and thereby controls the divergence of the metabolic pathways of saturated and unsaturated fatty acid synthesis in *E. coli* (Heath and Rock 1996). The product of dehydration (trans-2-decenoyl-ACP) is either released for subsequent reduction by FabI for the synthesis of saturated fatty acids or remains bound to FabA to be isomerized to cis-3-decenoyl-ACP. The double

bond isomerization occurs for the first time at the 10-carbon stage of fatty acid synthesis (Rock and Cronan 1996). Subsequently, the product of isomerization is condensed with acetyl-ACP by FabB, which conserves the double bond in the carbon chain and initiates the cycle of unsaturated fatty acid chain elongation. The rate of unsaturated fatty acid synthesis seems to be controlled by FabB (Clark et al. 1983). Consecutive cycles finally result in palmitoleic acid and cis-vaccenic acid (Gelmann and Cronan 1972), which represent unsaturated fatty acids in *E. coli*. Gram-positive bacteria lack enzymes like FabA and FabB and do not have a *de novo* metabolic pathway for unsaturated fatty acids. The unsaturated fatty acids are synthesized from existing saturated fatty acids and accomplished in a desaturation reaction (Aguilar et al. 1998).

The crystal structure of FabA from *E. coli* was determined in 1996 by Leesong et al. It is a soluble symmetric homodimer of two 171 amino acid long polypeptides (Cronan et al. 1988) with two independent active sites created by the dimer interface (Helmkamp et al. 1969, Schwab et al. 1985). The catalytic residues are a histidine from one subunit and an aspartic acid from the other subunit. Dehydration and isomerization seem to occur in the same active site (Helmkamp and Bloch 1969, Schwab et al. 1985).

Studies showed that a mutational inactivation of *fabA* or *fabB* genes results in an unsaturated fatty acid auxotroph phenotype (Silbert and Vagelos 1967, Rosenfeld et al. 1973). The fact that these mutants were still able to produce saturated fatty acids indicates that FabZ operates as additional dehydratase and FabF as an elongation-condensing enzyme in *E. coli* (Garwin et al. 1980, de Mendoza et al. 1983, Mohan et al. 1994). While FabA and FabZ show the same fold and 30 % sequence identity, there are differences in the active site residues: Histidine (H) and a carboxylic acid are the principal catalytic residues, but it is Aspartic acid (D) in FabA and Glutamic acid (E) in FabZ. Studies of FabA from *E. coli* and FabZ from *P. aeruginosa* showed that this switch is not responsible for the different catalytic properties, but rather the differences in the shape of the substrate binding pocket (Kimber et al. 2004, Lu et al. 2005). In 1967, it was shown that in the presence of 3-decynoyl-N-acetyl-cysteamine the enzyme is irreversible inactivated, despite the inhibitor showing different

stereochemistry than substrates or products (Kass and Bloch 1967). The allenic thiol ester alkylates the catalytic residue H70, (Cronan et al. 1988) resulting in a stable covalent enzyme inhibitor adduct (Helmkamp et al. 1969). While this structure has been determined (PDB 1MKA), the covalent modification alters the position of the inhibitor and therefore a structure of FabA or FabZ in complex with a correctly configured substrate has yet to be determined.

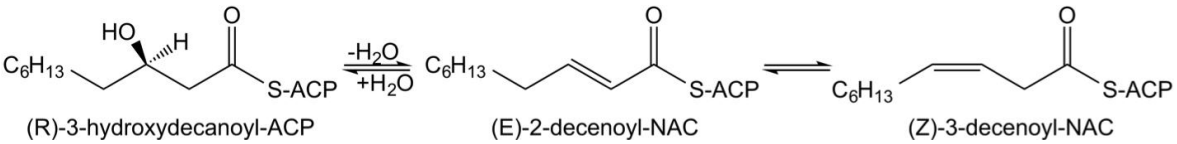

Figure 8: Catalytic reactions of FabA (Leesong et al. 1996). Biological reactions of dehydration and isomerization.

Similar to *E. coli*, *P. aeruginosa* has a FabA-FabB system for the biosynthesis of unsaturated fatty acids and a FabZ protein, which is not capable of isomerization (Hoang and Schweizer 1997). In 2004, Kimber et al. published the structure of FabZ from *P. aeruginosa* at 2.5 Å resolution (Kimber et al. 2004). Before starting this project, the structure of FabA from *P. aeruginosa* (*Pa*FabA) was solved in our lab (Figure 10). As anticipated, due to 70 % sequence identity the structure of *Pa*FabA looks similar to the FabA of *E. coli* (Figure 9). Structural alignment of the homologous FabA from *E. coli* (*Ec*FabA) with *Pa*FabA (rmsd of 0.58 Å for 166 Cα positions) suggested that the catalytic residues of *Pa*FabA would be H70 and D84.

```
E.coli          MVDKRESYTKEDLLASGRGELFGAKGPQLPAPNMLMMDRVVKMTETGGNFDKGYVEAELD 60
P.aeruginosa    -MTKQHAFTREDLLRCSRGELFGPGNAQLPAPNMLMIDRIVHISDVGGKYGKGELVAELD 59
                 : *:.::*:**** ..******. ..**********:**:*:::::.**::.** : ****

E.coli          INPDLWFFGCHFIGDPVMPGCLGLDAMWQLVGFYLGWLGGEGKGRALGVGEVKFTGQVLP 120
P.aeruginosa    INPDLWFFACHFEGDPVMPGCLGLDAMWQLVGFYLGWQGNPGRGRALGSGEVKFFGQVLP 119
                ********.*** ********************** *. *:***** ***** *****

E.coli          TAKKVTYRIHFKRIVNRRLIMGLADGEVLVDGRLIYTASDLKVGLFQDTSAF 172
P.aeruginosa    TAKKVTYNIHIKRTINRSLVLAIADGTVSVDGREIYSAEGLRVGLFTSTDSF 171
                *******.**:** :** *:::.:*** * **** **:*..*:**** .*.:*
```

Figure 9: Alignment of FabA proteins of *E. coli* and *P. aeruginosa*. Residues common to both proteins are indicated with an asterisk (*).

Therefore mutants of the catalytic residues were produced to allow for biochemical characterization and co-crystallization with a substrate analog. The additional information on how the substrate is bound in the active site should help with efforts to identify a molecule that inhibits *Pa*FabA and thus impair or inhibit the biosynthesis of fatty acids in *P. aeruginosa*. Since no other enzyme is able to adopt the function of *Pa*FabA it should lead to cytostasis or death.

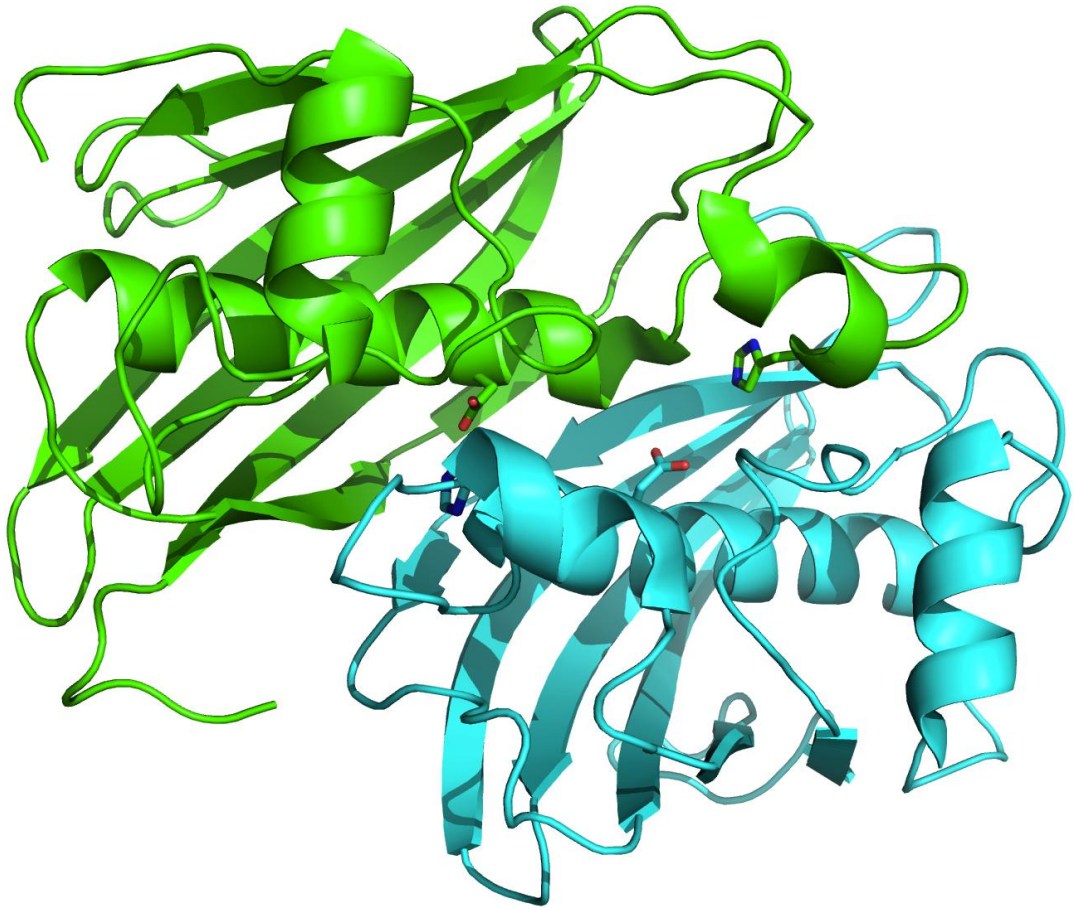

Figure 10: The structure of *Pa*FabA. Active site residues H70 and D84 are shown as sticks (Moynie et al. 2013).

1.8 Structure-based drug design

Since antibiotic resistance and nosocomial infections have become a serious problem in medicine today, there is an increasing interest to generate new antibiotics against Gram-negative bacteria.

Structure-based drug design is an important technique for the discovery of new drugs against specific targets. This method is based on the knowledge of the structure of a biological target obtained through methods like X-ray crystallography or NMR spectroscopy. The first successes of structure-based drug design were achieved after determination of the structures of the retroviral proteases RSV and HIV-1 in 1989. In 1990 Roberts discovered a peptide-based HIV protease inhibitor (Klebe 2000, Davis et al. 2003).

A drug target is most commonly a key molecule involved in a metabolic or signaling pathway. This pathway is specific to a disease condition or pathology, or to the infectivity or survival of a microbial pathogen. It is possible to target a key molecule, which inhibits the functioning of the pathway in the diseased state, or to enhance the normal pathway by promoting specific molecules, which may have been affected in the diseased state.

Structure-based drug design requires various steps. The first step includes cloning, purification and structure determination of the target protein or nucleic acid. Structure determination of macromolecules can be achieved by X-ray crystallography, NMR or in rare cases by homology modeling. The structure allows for the modeling of compounds or fragments from a library into a region of the structure that is considered to be biologically relevant, such as catalytic or allosteric sites. Based on steric and electrostatic interactions with the target site, the compounds are ranked and the most suitable compounds are tested with biochemical assays. Determining the structure of the target in complex with the small molecule can be used to guide further modification of the compound to increase its affinity for the target (Anderson 2003).

1.9 Aim

The worldwide increasing rates of multidrug-resistant *P. aeruginosa* call for the fast development of new antibiotic classes against this pathogen. The aim of this project was to extend our knowledge of the function and mechanism of the enzyme *Pa*FabA by biophysical and biochemical characterization. Research conducted is part of an ongoing project to discover a new antibiotic class

targeting this enzyme and thus influence the fatty acid metabolism of *P. aeruginosa.*

Four loss-of-function mutants of *Pa*FabA were expressed and purified and the structure of one such mutant was solved in its apo and holo forms. The stability of the mutants was analyzed in comparison to the wild-type protein by fluorescence-based thermal shift assays and the activities of the mutants were studied using UV-spectrophotometry.

2 MATERIALS ANS METHODS

2.1 Materials

2.1.1 Reagents

20× NPS	0.5 M $(NH_4)_2SO_4$ (Fluka) 1 M KH_2PO_4 (Fisher) 1 M Na_2HPO_4 (Sigma) in double-distilled (dd) H_2O
50× 5052	25 % glycerol (Riedel de Haen) 2.5 % glucose (Sigma) 10 % α-lactose (Sigma) in dd H_2O
Acetic Acid	Sigma
Agarose	Sigma
Ammonium sulfate	Fluka
Ampicillin sodium salt	Sigma
Sodium hydroxide	Sigma
Citric acid	Sigma
Complete EDTA-free protease inhibitors	Roche
Coomassie Brilliant Blue R-250	BDH
Coomassie staining	50 % Methanol (Fisher)

	40 % H_2O
	10 % Acetic Acid (Fisher)
	2.5 g R-250 (BDH)
D-(+)-glucose	Sigma
Dipotassium phosphate	Fisher
Dimethyl sulfoxide (DMSO)	Sigma
Dithiothreitol (DTT)	Formedium
Ethylenediaminetetraacetic acid (EDTA)	Sigma
Ethanol	Fisher
Glycerol	Riedel de Haen
Hydrochloric acid	Sigma
Imidazole	Sigma
Isopropyl β-D-1-thiogalactopyranoside (IPTG)	Sigma
Lithium sulfate	Sigma
Magnetic Ni-Particles	Promega
Magnesium chloride	Sigma
Methanol	Sigma
NuPage Novex Bis-Tris Mini Gels	Invitrogen
PEG 4.000	Fluka
PEG MME 5.000	Fluka
Potassium dihydrogen phosphate	Fisher
Precision Plus Protein Unstained Standards	BioRad
2x Sample buffer, Laemmli	Sigma
Sodium azide	Riedel-de Hain
Sodium chloride	Sigma
Sodium citrate	Sigma
Sodium fluoride	Sigma
Sodium phosphate dibasic	Sigma
Sodium phosphate monobasic	Sigma

5000x SYPRO® Orange protein gel stain	Invitrogen
Tricine	Sigma
Tryptone	DUCHEFA
Urea	Melford
Yeast extract	DUCHEFA
ZY	1 % N-Z-amine AS (Sigma) 0.5 % yeast extract (DUCHEFA) in H_2O
α-Lactose	Sigma

2.1.2 Devices and other instruments

Cell disrupter	Constant flow cell disrupter	Constant Systems Ltd.
Chromatography system	ÄKTAxpress	GE Healthcare
Filter (0.45µm)		Millipore
Ni-column	HiTrap IMAC	GE Healthcare
Desalt column	HiPrep 26/10 Desalting	GE Healthcare
Protein Concentrator, 10kDa MWCO	Viaspin	Satorius Stedim
Gel filtration column	HiLoad 16/60 Superdex™ 200 prep grade	GE Healthcare
Pre-crystallization test		Hampton Research
Crystallization robot	Honeybee	Cartesian
Centrifuge	Evolution RC	Sorvall
	Avanti J-20XP	Beckman Coulter
	Multifuge 3SR+	Heraeus

	Legend RT	Sorvall
	5417R	Eppendorf
	Biofuge Pico	Heraeus
Sonicator	Soniprep 150	MSE
Automated small-scale purification machine	BioSprint 15	Qiagen
Water bath	QBD2	Grant
Thermofluor machine	MX3005P	Stratagene
SDS-PAGE power pack	Power Ease 500	Invitrogen
SDS-PAGE gel tank	Xcell SureLock Mini-Cell	Invitrogen
Microwave		Cookworks
pH-meter		
Spectrophotometer	Nanodrop 1000	Thermo Scientific
Incubator	HAT Multitron Standard	Infors
	Innova 4400	New Brunswick
	Innova 4430	New Brunswick
CD machine	J-810 spectrophotometer	Jasco
CD cuvettes	Near 110-QSP	
	Far 121.000-QSP	
UV-visible spectrophotometer	Cary 50 Bio	Varian
UV cuvettes	18BMUV10	Precision Cells Inc.

2.1.3 Cells

BL21star (DE3) Competent *E. coli*	Invitrogen
Tuner (DE3) Competent *E. coli*	Novagen

2.1.4 Culture medium

Lysogeny broth (LB)	1 % Tryptone 0.5 % Yeast Extract 171 mM NaCl
Tryptone phosphate broth (TPB)	2 % Tryptone 12 mM K_2HPO_4 15 mM KH_2PO_4 86 mM NaCl
LB/Ampicillin plates	99 % LB-medium 1 % agarose 100 µg/mL Ampicillin
ZYP-5052 rich medium for auto-induction	For 400 mL medium: ZY containing 1 mM $MgSO_4$ 1x 5052 1x NPS 100 µg/mL Ampicillin

2.1.5 Enzymes

Lysozyme from chicken egg white	Fluka
DNAse from bovine pancreas	Sigma
His_6-tagged tobacco etch virus (TEV) protease	In house expression and purification

2.1.6 Buffers

Lysis buffer (A)	20 mM sodium phosphate pH 7.4 500 mM NaCl 10 % glycerol 10 mM imidazole
Wash buffer (W)	20 mM sodium phosphate pH 7.4 500 mM NaCl 10 % glycerol 30 mM imidazole
Elution buffer (E)	20 mM sodium phosphate pH 7.4 500 mM NaCl 10 % glycerol 300 mM imidazole
Low salt (LS) buffer	10 mM Tris pH 7.5 150 mM NaCl
Phosphate buffer	50 mM sodium phosphate pH 7.5 150 mM NaF

2.2 Methods

2.2.1 Transformation

Transformation is the genetic alteration of a cell through the uptake of plasmid-DNA into prokaryotic cells like *E. coli*. Heat shock method was used to permeabilize the membrane and cause penetration of the DNA into the bacterium.

Full-length *Pa*FabA was cloned previously in the lab with an N-terminal TEV protease cleavable His6-tag in pDEST14 (Invitrogen). The mutations H70Q, H70N, D84N and H70N/D84N were performed in the lab using a modified

protocol of Quickchange method (Liu and Naismith 2008) and mutations confirmed using DNA sequencing.

The pDEST14 expression vectors were transformed into chemically competent BL21 star cells or Tuner cells. Cells and DNA were thawed on ice. 10-100 ng of DNA was added to 50 µL of cells and the mixture incubated on ice for 30 minutes. DNA uptake was caused by heat shock for 75 seconds in a water bath at 42 ºC. Afterwards, cells were placed on ice for 10 minutes and 950 µL pre-warmed LB medium was added to the cells, which were then incubated at 37 ºC and 200 rpm for 60 minutes, before being plated on a LB agar plate containing ampicillin. The plates were incubated at 37 ºC overnight.

2.2.2 Small-scale expression and purification

Small-scale expression and purification experiments were performed initially to judge the effects of different growth conditions on expression levels and solubility of the proteins.

Small-scale expression experiments were performed in LB, TPB and ZYP-5052. For trials with LB and TPB growth media, 10 mL media was supplemented with 100 µg/mL ampicillin (final concentration) and inoculated with a single colony. These cultures were incubated overnight at 37 ºC and 200 rpm. Subsequently, 100 mL growth media supplemented with ampicillin was inoculated with the overnight culture (1:100 dilution) and incubated at 37 ºC and 200 rpm until mid-log growth phase (OD_{600}~0.6-0.8). OD_{600} indicates the absorbance, or optical density, of a sample measured at a wavelength of 600 nm. It is a method for estimating the concentration of cells in a liquid. Protein expression was induced by the addition of 0.4 or 1 mM IPTG and the cells were incubated at 37, 25, 20 or 15 ºC for 3 h or overnight.

For auto-induction media (ZYP-5052), a single colony was used to inoculate 200 mL LB media containing 100 µg/mL ampicillin and 1 % glucose. The culture was incubated at 37 ºC and 200 rpm overnight. Subsequently, 400 mL ZYP-

5052 medium was inoculated with overnight culture (1:80 dilution) and incubated at 20 ºC and 250 rpm before harvesting after approximately 48 hours. Cultures were harvested by centrifugation at 4,000 g at 4 ºC for 20 min. The cell pellets were resuspended in 1 mL buffer A and lysed mechanically by sonication for 2x 7 s at 7 microns on ice. To remove cellular debris and insoluble protein, the lysate was centrifuged at 21,000 g and 4 ºC for 10 minutes. The supernatant was analyzed using the BioSprint 15 workstation using buffers W and E according to manufacturer`s instructions (Qiagen). The eluates were analyzed by Sodium Dodecyl Sulphate Polyacrylamide Gel Electrophoresis (SDS-PAGE).

2.2.3 SDS-PAGE

SDS-PAGE is a technique used to separate proteins according to their molecular weight.

2× SDS-PAGE sample buffer was added to the protein sample (1:1) and boiled for 3 minutes at 100 ºC. The samples were loaded onto Pre-cast NuPage Novex 4-12 % Bis-Tris Mini Gels. Precision Plus Protein Unstained Standards were also loaded to allow for molecular weight estimation. The electrophoresis was executed in an XCell Surelock Mini-Cell filled with 1×SDS MES Running Buffer and run for 35 min at 200 V using a Power Ease 500 power pack. The gels were stained using Coomassie and destained in boiling water.

2.2.4 Large-scale expression and purification

Proteins were expressed as described above by overexpression in *E. coli* BL21 star cells using 4 L liquid culture per construct ZYP-5052 rich medium for auto-induction. Cells were harvested by centrifugation at 8,000 x g and 4 ºC for 10 min.

Pellets were resuspended in buffer A (5 mL buffer per 1 g wet pellet). The buffer was supplemented with 20 µg/mL DNAse, 1 mg/mL lysozyme and EDTA-free protease inhibitor tablets (1 tablet per 50 mL buffer). The mixture was stirred for 20 minutes at 4 ºC until the pellet was completely resuspended. The cells were lysed using a Constant Flow cell disruptor at 30 kpsi and the lysate was spun down at 50,000 x g and 20 ºC for 20 min. The supernatant was passed through a 0.45 µm filter and applied to a 5 mL Ni immobilized metal affinity chromatography (IMAC) HiTrap column using an ÄKTAxpress system at 5 mL min^{-1}. The column was washed with buffer W and the protein was eluted with a single step using buffer E at 5 mL min^{-1}. The eluate was applied to a HiPrep 26/10 desalting column using buffer W for buffer exchange and imidazole removal at 10 mL min^{-1}. TEV protease was then added at a ratio of 1:10 protease-protein to cleave the His_6-tag. After 1 h at 20 ºC the completeness of cleavage was analyzed by SDS-PAGE. After >90 % of the protein was cleaved, the solution was passed over a second Ni IMAC HiTrap column in the same buffers at 5 mL min^{-1} used for the first Nickel column to remove the cleaved His_6-tag, His-tagged TEV protease and other contaminants. The flow-through was collected and concentrated using a Vivaspin concentrator at 4,000 x g and 4 ºC. The sample was then applied to a Superdex™ 200 16/60 gel filtration column equilibrated in buffer LS at 1 mL min^{-1} to separate the target protein from aggregates and contaminants. Subsequently, protein was concentrated to a final concentration of 6 mg/mL.

2.2.5 Crystallography

Interpreting the diffraction patterns of X-rays scattered by the atoms in a crystal is the only method to obtain high-resolution structures of a macromolecules. Currently, the Protein Data Bank (PDB) is the repository of macromolecular models obtained from experimental data. It contains more than 64,000 structures of proteins and nucleic acids determined by X-ray crystallography.

Like any molecule in a crystal lattice, proteins adopt regular organization when they enter into the crystalline state. Primarily hydrogen bonds between hydrated protein surfaces cohere the protein crystal, but salt bridges and hydrophobic interactions can also contribute. The method of vapor diffusion is often used for growing protein crystals. Purified protein is added to an aqueous buffer containing a precipitant at a concentration necessary to precipitate the protein. Water is then removed by vapor diffusion between the protein solution and a reservoir solution of the precipitant to increase the concentrations of protein and precipitant, resulting in “ordered precipitation” from a supersaturated solution. Protein-ligand complexes can be obtained by co-crystallization where the complex is crystallized from a protein solution containing the substrate. Crystals are mounted by picking them up in a loop of glass wool, steel, synthetic fiber, nylon or plastic. Before flash freezing the crystals to limit radiation damage during data collection by dipping the loop into liquid nitrogen, crystals were cryoprotected to prevent the formation of ice crystals, which strongly diffract x-rays.

To estimate the optimal protein concentration for use in crystallization trials, the pre-crystallization test (Hampton research) was used. The Cartesian Honeybee was used to screen through several prepared sets of random sparse matrix crystallization screens. The experiments were set up as sitting drops in 96-well crystallization plates. Drops consisted of 0.15 µL protein and 0.15 µL precipitant or 0.3 µL protein and 0.15 µL precipitant. The screening experiments were incubated at 20 ºC. Mutants were screened both as pure protein and co-crystallized with the substrate mimics 3-hydroxydecanoyl-NAC and (*E*)-2-decenoyl-NAC. These substrate mimics were synthesized in house. For co-crystallization 1mM of the substrate dissolved in DMSO was added to the protein sample and incubated for two hours before the plates were set up. Subsequently, crystal optimizations were carried out around the initial crystal hits generated by the screening experiments. Optimized crystals were grown in 25 % PEG 4000, 0.1 M sodium citrate pH 5 and 0.05 M ammonium sulfate at 20°C and were cryoprotected in mother liquid supplemented with 15 % glycerol. Diffraction data were collected at 100 K on the ID29 beamline of the ESRF. A

PILATUS was used to record the images of the X-rays diffracted by the crystal. Recorded diffraction spots were integrated to calculate spot intensities with XDS (Kabsch 2010), which were then scaled and merged using Scala (Evans 2006). Intensities were converted to structure factors with Ctruncate. Since a similar structure had already been solved, data from Ctruncate could be used as a search model for molecular replacement with PHASER (McCoy et al. 2007), which uses rotation and translation functions to calculate phases. The result is an electron density map a protein model can be built into.

2.2.6 Fluorescence-based Thermal Shift Assay

The Fluorescence-based Thermal Shift Assay is a technique used to determine thermal stability of proteins and to identify factors influencing this stability. It utilizes an environmentally sensitive fluorescent dye (typically SYPRO® Orange) to observe thermal unfolding of the protein. The dye has an affinity for hydrophobic parts of the protein, which are exposed as the protein undergoes unfolding. The increasing fluorescence signal of the dye as the protein unfolds can be used to measure the temperature at which the protein unfolds. There is a relationship between the stability of a protein and its Gibbs free energy of unfolding (ΔGu). When the temperature increases and the protein becomes less stable, ΔGu decreases and becomes zero at equilibrium where the amounts of folded and unfolded protein are equal. At this point, the temperature is called melting temperature (T_m), shown as the midpoint of the unfolding transition in the melting curve. It can be calculated using the Boltzmann equation:

$$y = LL + {}^{(UL-LL)}/1+\exp(T_m - x/a)$$

LL= value of minimum intensity

UL= value of maximum intensity

a= slope of the curve within T_m

A shift in T_m under different conditions indicates an alteration in stability. Ingredients such as buffers, additives and salts can be screened to determine if

they have an impact on a protein's thermal stability, as seen as a change in the T_m. A binding ligand can show an effect on the melting temperature as well. The Stratagene Mx3005P qPCR system was used to automatically monitor the thermal melting profiles of the proteins under different conditions.
1 µl SYPRO® Orange (2.5x final concentration) and 5 µg protein was added to various buffers in a 96-well plate with a final volume of 25 µl. The plates were sealed and centrifuged at 340 g and 18 ºC for 2 min, before starting the experiment using Stratagene Mx3005P. Every condition was tested at least in triplicate. Additionally, three wells were used as a control without the protein to ensure that the ingredients of the buffer had no effect on the dye. The T_m was calculated using GraphPad Prism 5.

2.2.7 UV spectrophotometry

For UV spectrophotometry and circular dichroism experiments the buffer was changed by dialysis to a buffer of low absorbance in the region of the wavelength of maximum absorbance of (E)-2-decenoyl-NAC (260 nm) and of the far-UV spectrum (260-180 nm). The buffer containing 10 mM Tris pH 7.5, 150 mM NaCl was replaced by a buffer containing 50 mM sodium phosphate pH 7.5, 150 mM NaF. Dialysis was carried out in Slide-A-Lyzer dialysis cassette at 4 ºC overnight.
UV-spectrophotometry is routinely used in analytical chemistry to determine the quantity of several absorbing species such as organic compounds or biological macromolecules. The Beer-Lambert law states that the absorbance of a solution is proportional to the path length through the sample (l), the concentration of the absorbing substance in the solution (c) and the extinction coefficient (ε): $A=l\times c\times \varepsilon$.

UV-spectrophotometry was used to determine the activity of the enzyme and to compare its activity to the activity of the mutants. Measurements were performed on a Varian Cary-50, Bio Spectophotometer (Varian, Inc.) using quartz cuvettes with a path length of 1 cm. This assay is based on the fact that

only the (E)-2-decenoyl-NAC absorbs at 260 nm because of its conjugated double bonds (Figure 11). 250 µL buffer and 250 µL water was used to blank. 250 µL buffer was supplemented with 14 µg protein, 0.3 mM 3-OH-decanoyl-NAC or 0.1 mM (E)-2-decenoyl-NAC and water to a final volume 500 µl. Subsequently, the protein concentration was increased up to 40 µg. Each solution was measured in three replicates.

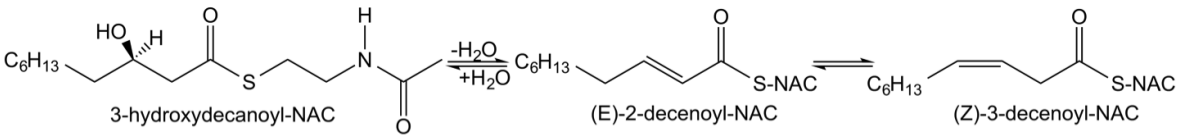

Figure 11: Chemical structures of substrate analogs, which mimic the ACP substrates.

2.2.8 Circular Dichroism

Circular Dichroism (CD) measures the differences in the absorption of left-handed polarized light against right-handed polarized light, which arise from structural asymmetry of the chiral protein. A spectrum resulting from an ordered structure can contain positive and negative signal.

The far-UV spectral region (190-250 nm) can be used to determine the secondary structure of the protein. The peptide bond is the chromophore at these wavelengths. The signal arises when the peptide bond is located in a regular, folded environment. α-helix, β-sheet and random coil structures each lead to characteristic shapes of CD spectrum.

Using the CD spectrophotometer JASCO 8.10 and the software Spectra Manager, a scan rate of 50 nm/min and a maximum response time of 0.6 s were used. A cylindrical cuvette with a path length of 0.5 mm was loaded with 200 µL of the sample at a concentration of 1 mg/mL. Before protein samples were loaded, a blank spectrum was run with the relevant buffer. For each sample eight scans were performed and subsequently averaged into a single spectrum by the software to improve the signal-to-noise ratio.

3 RESULTS

3.1 Expression and purification of *Pa*FabA mutants H70Q, H70N, D84N and H70N/D84N

The catalytic residues of *Pa*FabA were predicted to be H70 and D84. Therefore four conservative mutants (H70N, H70Q, D84N, and H70N/D84N) were designed to probe the catalytic site of the protein. Protein yields of wild-type enzyme and mutants were very poor. Therefore the first goal was to optimize the expression conditions of the mutants. Two *E.coli* strains, temperatures, media, IPTG concentrations and incubation times were tried. Every condition was evaluated in small-scale (10 mL) cultures and analyzed using the Biosprint 15. The mutants were expressed in Tuner and BL21 Star cells with LB, TPB and ZYP-5052 media at 15, 20, 25 and 37 °C. Initial attempts using LB or TPB media resulted in good expression but very little soluble protein which could be used for further experiments (Figure 13). Expression at different temperatures had little effect on the amount of soluble protein. A selection of different expression conditions is shown in Figure 12 for the double-mutant H70N/D84N. The optimal expression conditions for wild-type *Pa*FabA were Tuner cells in LB medium at 15 ºC overnight with induction by 0.4 mM IPTG. For all mutant proteins the largest amounts of soluble protein were detected using BL21 Star cells and auto-induction (ZYP-5052) medium with incubation at 20 ºC for 48 h (Figure 13).

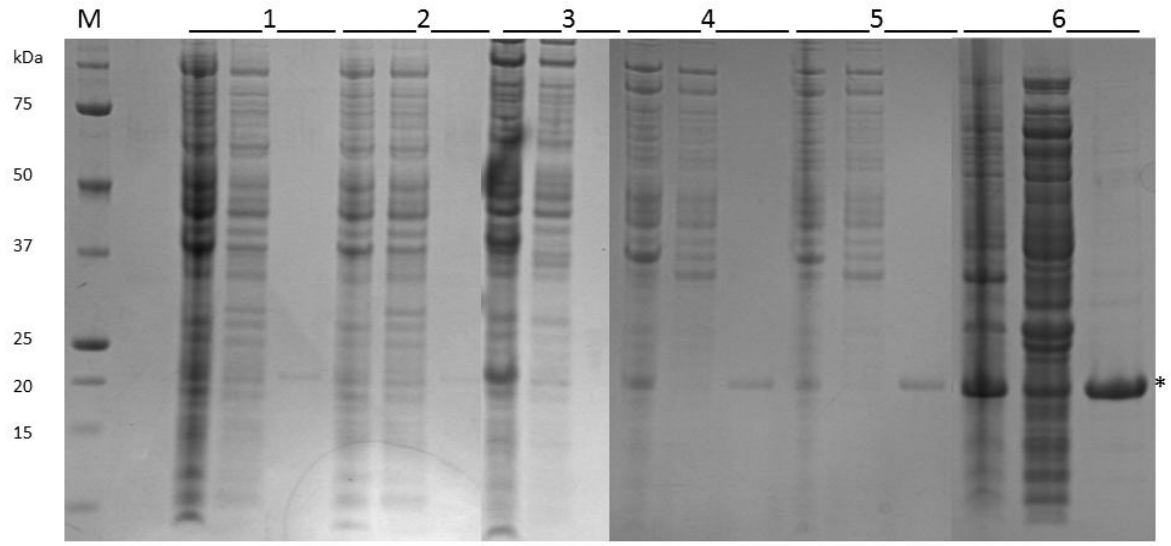

Figure 12: SDS-PAGE of small-scale expression trials of *Pa*FabAH70N/D84N (18.7 kDa) using the Biosprint 15 system (section 2.2.2). For each condition the insoluble (left), flow-through (middle) and eluate (right) fractions are shown. M: protein standard markers. 1: Tuner cells, LB medium, 0.4 mM IPTG, 37 ºC for 3 h; 2: Tuner cells, LB medium, 1 mM IPTG, 25 ºC for 3 h; 3: BL21Star cells, TPB medium, 0.4 mM IPTG, 37 ºC for 3 h; 4: BL21 Star cells, LB medium, 0.4 mM IPTG, 37 ºC for 3 h; 5: BL21 Star cells, LB medium, 0.4 mM IPTG, 37 ºC for 4 h; 6: BL21 Star cells, ZYP-5052 medium, 20 ºC for 48 h. The * indicates the expected molecular weight of the protein of interest. Type and treatment of all SDS-PAGE gels found in this body of work can be found in section 2.3.3.

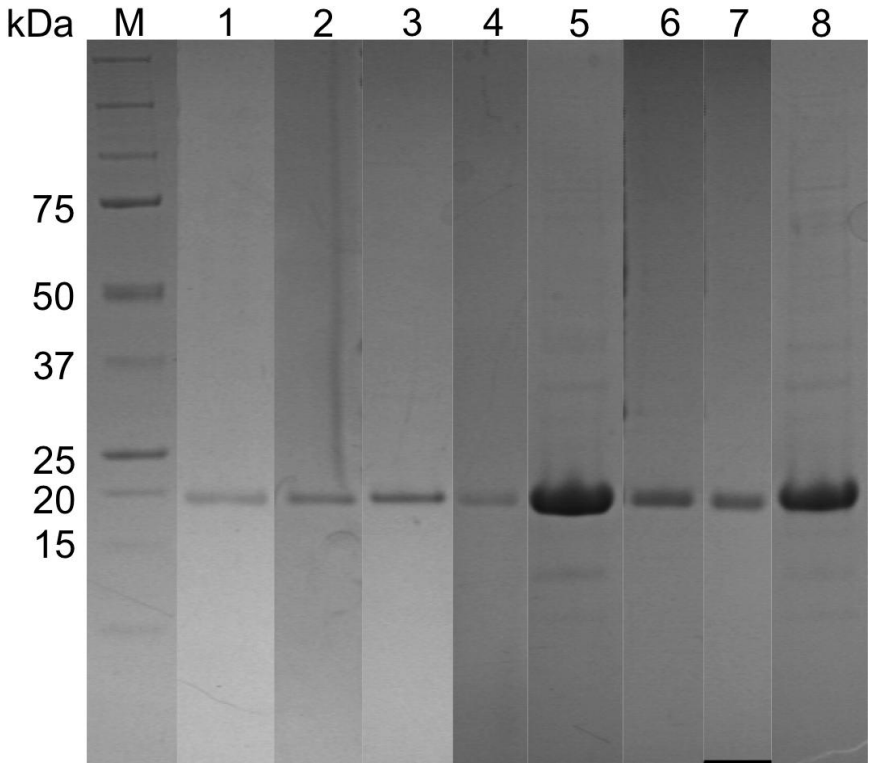

Figure 13: Comparison of protein expression in LB and auto induction medium. SDS-PAGE of small-scale expression trials of the four investigated *Pa*FabA mutants (18.7 kDa) in BL21 Star cells after Ni^{2+}-pull-down. 1-4: Expression of mutants H70Q (1), H70N (2), D84N (3) and H70N/D84N (4) at 37 ºC for 3 h in LB medium. 5-8: Expression of mutants H70N (5), H70Q (6), D84N (7) and H70N/D84N (8) in ZYP-5052 medium at 20 ºC for 48 h.

Since ZYP-5052 medium gave by far the most protein for all mutants large-scale expression was carried out using BL21 Star cells and ZYP-5052 medium as described in the Materials and Methods section. The average biomass from 800 mL of culture was 15 g wet pellet. Purification was performed as described in three steps: an initial Ni-NTA affinity chromatography followed by TEV cleavage to remove the His_6-tag, a second Ni-NTA affinity step and finally gel filtration.

Purifications of all four mutants were identical and provided protein, although the yield varied by as much as two-fold between mutants. A representative purification for *Pa*FabAH70N is shown below. 28 g wet pellet from 1.5 L of cell culture was used for this purification. The pellet was resuspended and lysed by sonication. 5 µL samples were taken at all appropriate stages and analyzed by SDS-PAGE to monitor the purifications. Whole cell lysate and insoluble protein

pellet analyzed on SDS-PAGE showed that > 50 % of target protein was in the soluble fraction (Figure 14(B)). The supernatant was passed over a Ni-IMAC column. The sample contained enough soluble target protein to exceed the column protein binding capacity. Most impurities were removed during a 30 mM imidazole wash. No detectable amount of *Pa*FabAH70N was washed off the column during this stage. Step elution with 300 mM imidazole in the same buffer yielded a sharp peak (Figure 14(A)). The UV absorption does not return to baseline because of impurities in the imidazole used.

(A)

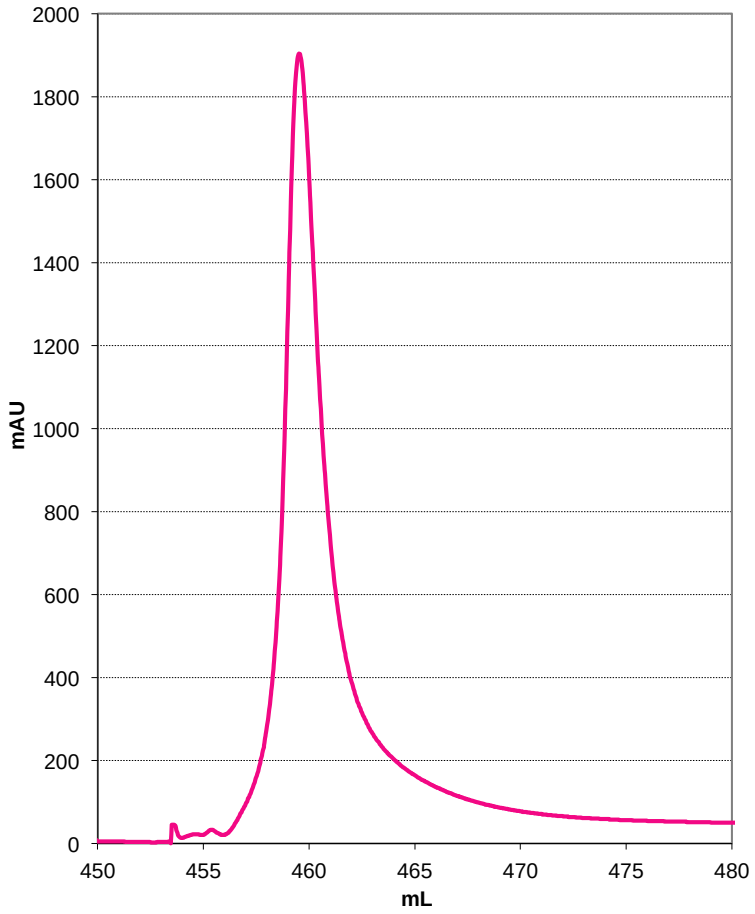

(B)

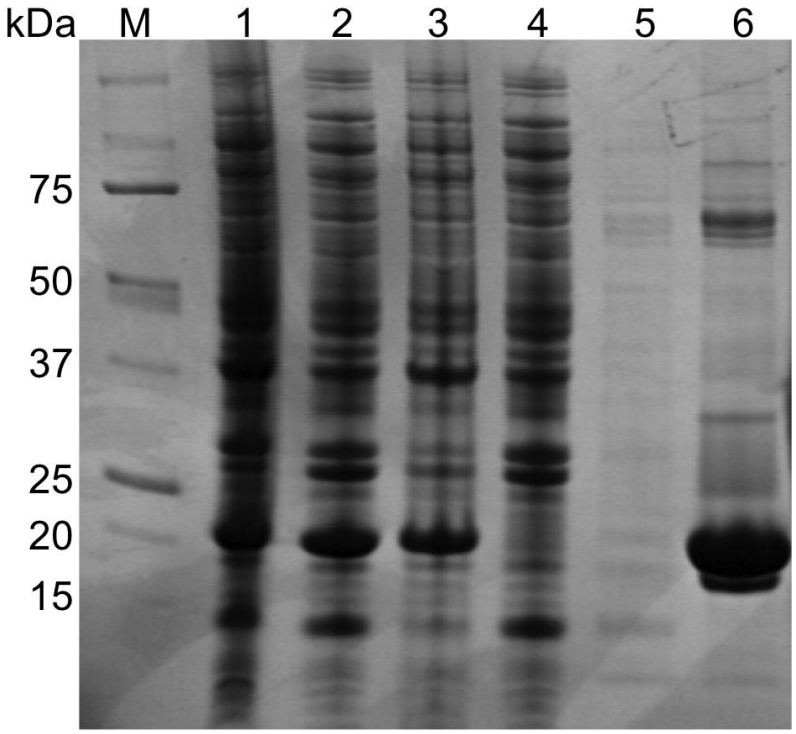

Figure 14: First Ni-IMAC affinity purification step of *Pa*FabAH70N. (A) UV absorbance (280 nm) of protein being eluted off the Ni-IMAC column, which was processed as described in 2.2.4. (B) SDS-PAGE of whole cells (1), supernatant (2), insoluble fraction (3), Ni flow-through (4), wash (5), and elution (6).

The peak elution fractions from Ni-IMAC were combined and the imidazole removed by passing the protein over a desalting column equilibrated with buffer W supplemented with 1 mM DTT and 0.5 mM EDTA. Imidazole removal is essential for TEV protease activity. The peak fractions were combined and the measured protein yield was 269 mg.

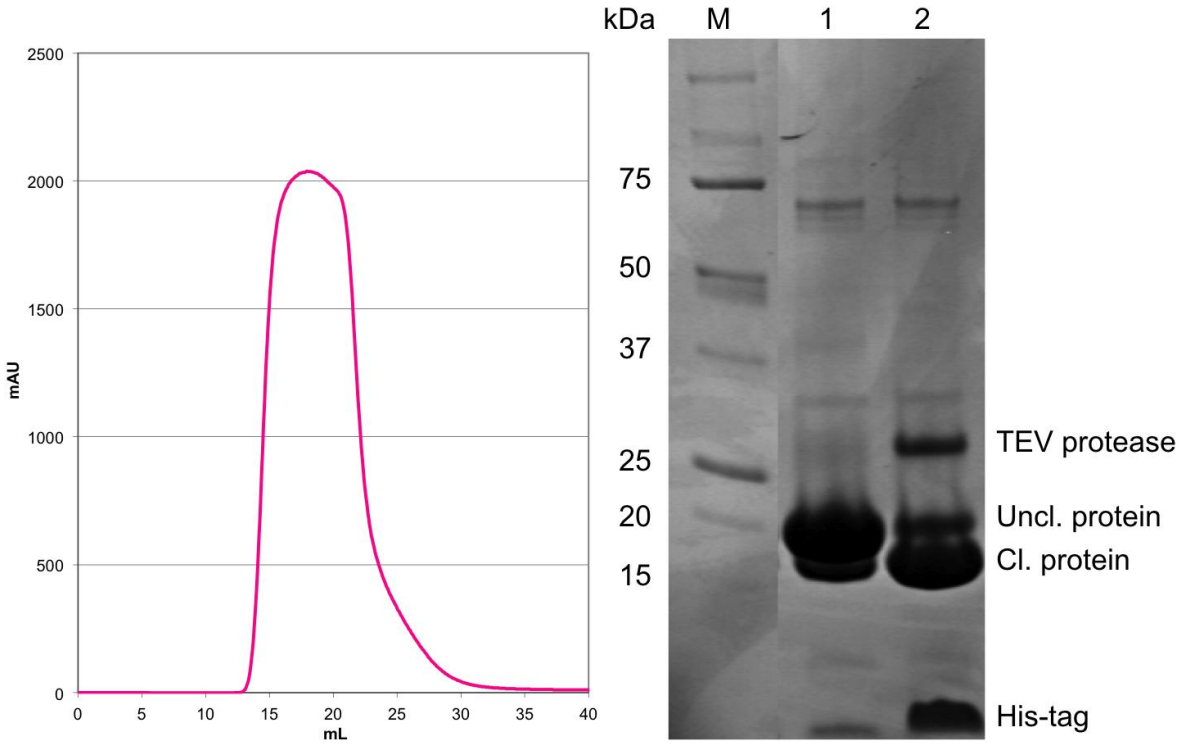

Figure 15: Desalting (Buffer exchange) of protein eluted from a Ni-IMAC column for imidazole removal and subsequent TEV-cleavage reaction. (A) UV absorbance (280 nm) of protein during buffer exchange on a desalting column (2.2.4). (B) SDS-PAGE of protein after desalting (1) and after TEV cleavage (2). TEV protease and products of the cleavage reaction are labeled. Uncl (unncleaved protein), Cl (cleaved protein).

13 mg of His_6-tagged TEV protease (mass ratio of 1:20, protease-to-protein) was added to cleave the N-terminal His_6-tag off *Pa*FabAH70N. After 1 h incubation at room temperature the mixture was analyzed by SDS-PAGE to confirm completion of cleavage. As can be seen in Figure 15, cleavage was mostly complete after one hour and the sample passed over a second Ni-IMAC column to remove the cleaved His_6-tag, TEV protease and contaminants (Figure 16). The vast majority of *Pa*FabAH70N was in the flow through. To ensure that no target protein was bound to the column we applied a step elution phase with 300 mM imidazole. Elution fractions contain mostly contaminants, TEV protease and trace amounts of uncleaved protein.

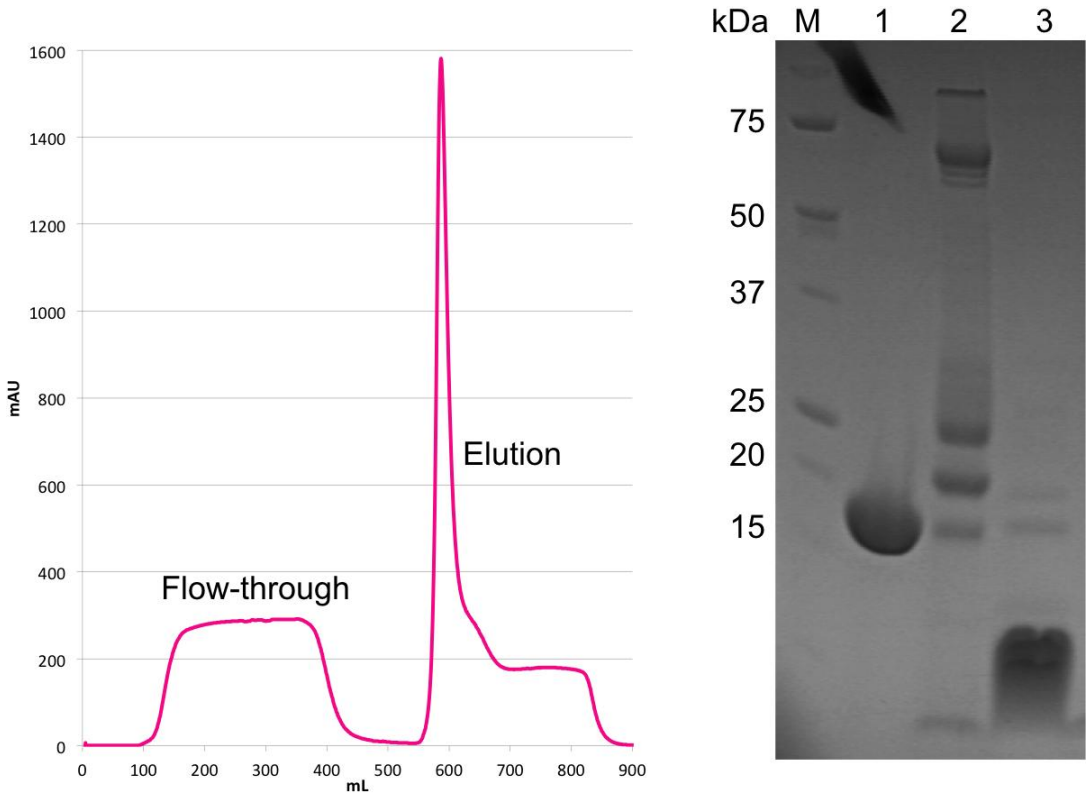

Figure 16: Second Ni-IMAC affinity step during *Pa*FabAH70N purification for the removal uncleaved protein, TEV protease and His_6-tag. (A) UV absorbance (280 nm) of protein passing over a 2nd Ni-IMAC column and step elution. Digested protein from which the His-tag was removed is now in the flow-through and was collected. The elution peak contains TEV protease, uncleaved protein and the cleaved His-tag. Details can be found in section 2.2.4. (B) SDS-PAGE of protein in the flow-through (1, cleaved protein) and from the elution fractions (2 and 3 TEV protease, impurities and cleaved His_6-tag).

All flow-through peak (plateau) fractions were combined and the yield was 245 mg of protein. Before gel filtration, the sample was concentrated to a final volume of 15 mL. A Superdex 200 16/60 column was equilibrated with buffer LS and 7.5 mL of protein were passed over the column per run (Figure 17). The protein was purified to homogeneity (as determined by SDS-PAGE) with a final yield of 161 mg (105 mg/L culture). Subsequently, the sample was concentrated to a final concentration of 6 mg/mL.

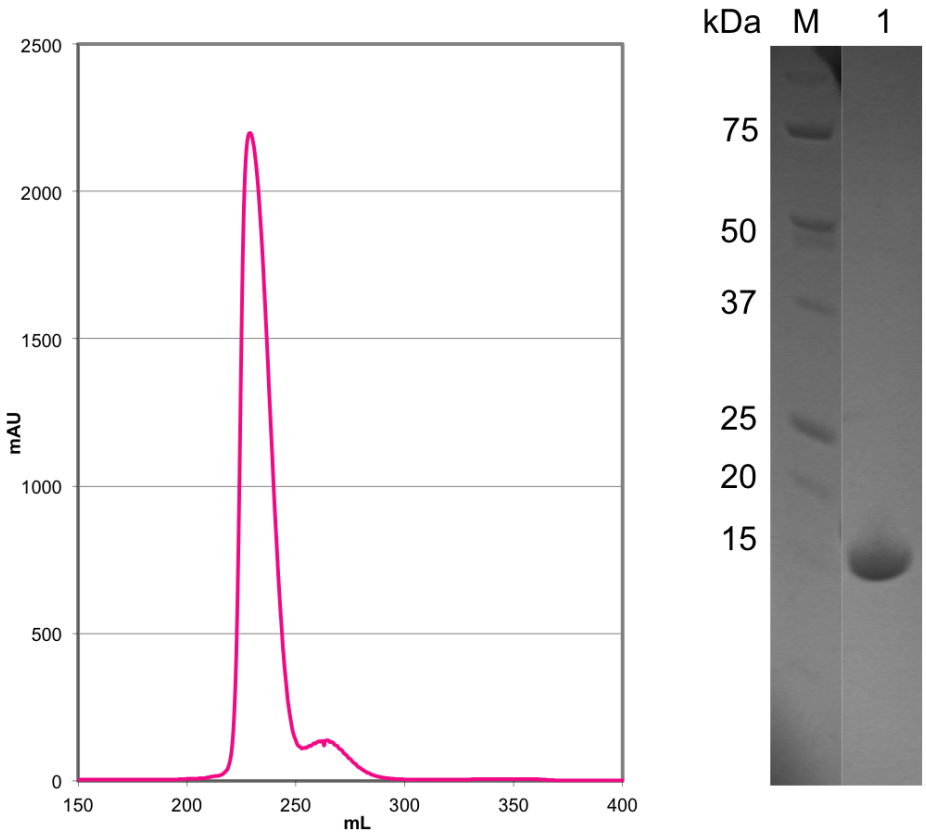

Figure 17: Size exclusion chromatography (SEC, or "gel filtration") of *Pa*FabAH70N. (A) The flow-through (Cleaved protein, Fig. 16) was concentrated and loaded onto a SEC column. UV absorbance (280 nm) of gel filtration run showing a sharp, symmetrical peak for the target protein. Details can be found in section 2.2.4. (B) SDS-PAGE of combined fractions after gel filtration (or SEC) (1). No contaminants were detectable using Coomassie stain.

Comparing the traces of the gel filtration runs of the different mutants and the wild-type protein (Figure 18) show that D84N elutes similar to wild-type protein while the other three mutants are shifted to an earlier elution volume. According to calibration curves of the column all proteins still eluted at a volume corresponding to approximately 45 kDa within an acceptable margin for error. This indicates that all mutants are tightly associated solution dimers like the wild-type protein. Mutant H70Q was partly aggregated when applied to the gel filtration column and the aggregated protein was removed during this step.

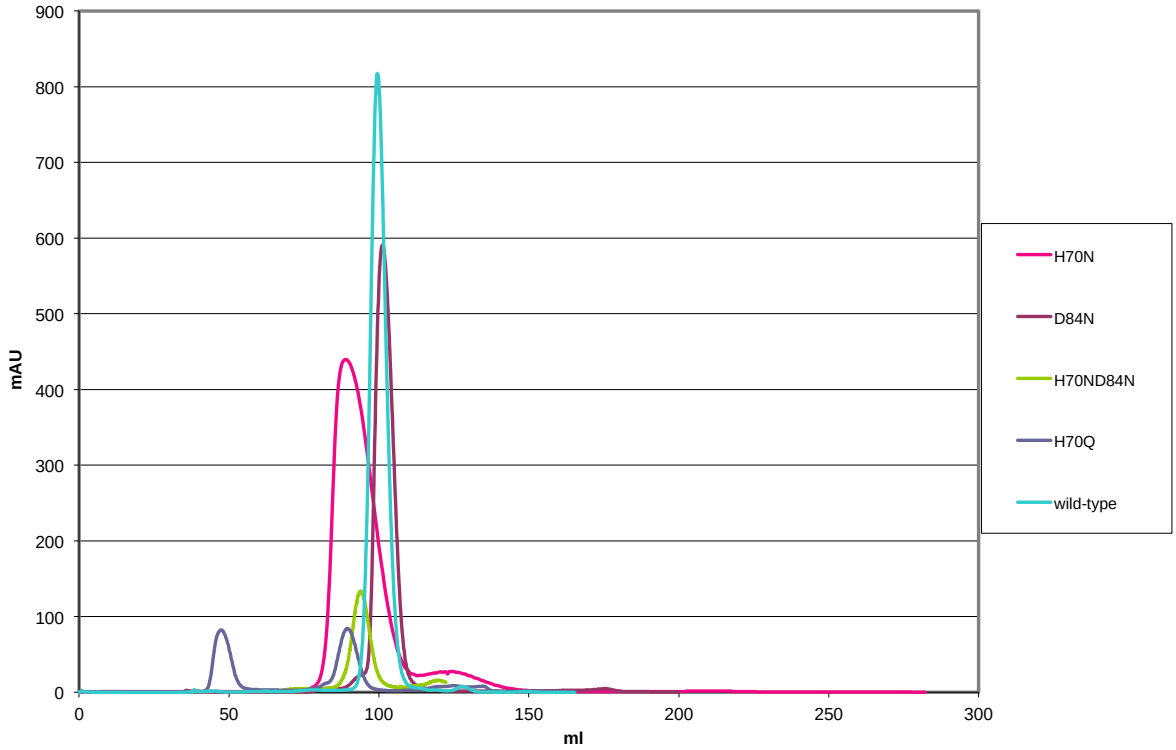

Figure 18: Gel filtration traces of *Pa*FabA wild-type and all four mutants. All protein elute at approximately the same volume. The peak at 50 mL for *Pa*FabAH70Q is caused by partial aggregation.

3.2 Biochemical and biophysical characterization of the mutants and the wild-type

In order to characterize the enzyme and its four mutants we used three assays. Our first concern was whether the introduced mutations disrupted protein folding. While similar behavior to wild-type protein during gel filtration was indicative of properly folded mutants, we recorded the circular dichroism (CD) spectra of all five proteins (Figure 19).

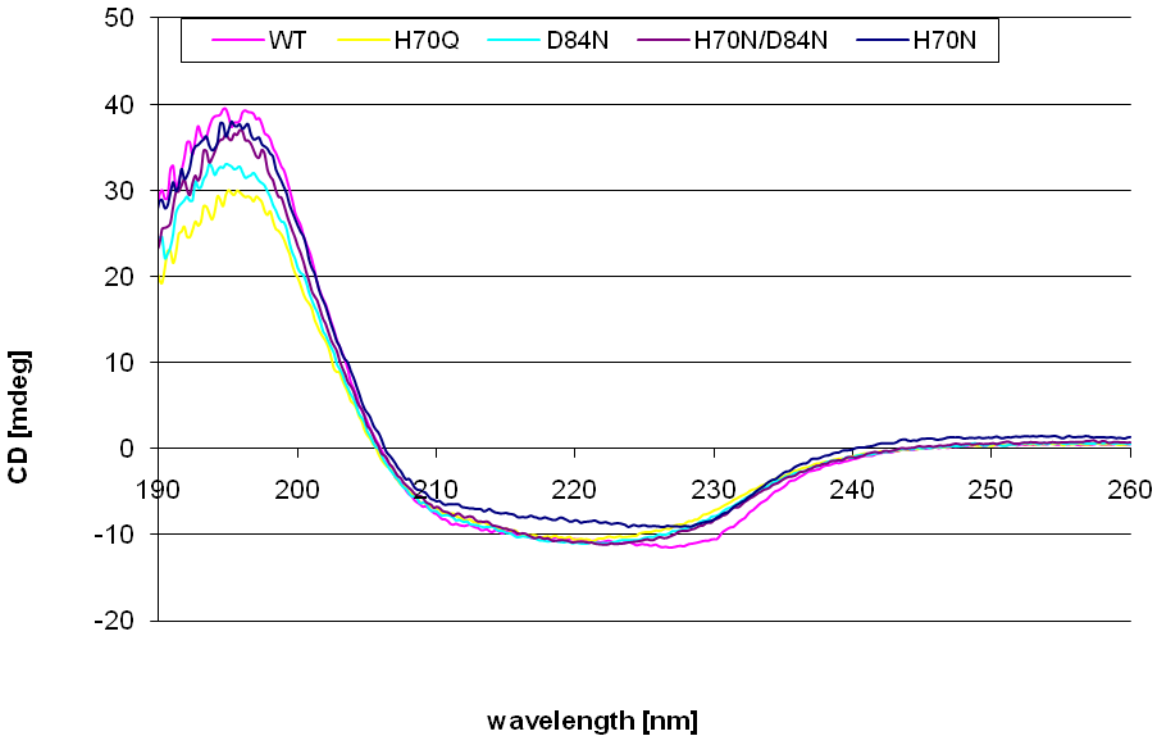

Figure 19: Far-UV CD spectra for wild-type *Pa*FabA and four mutants. All five proteins show highly similar spectra, indicating similar folds.

As expected from gel filtration, the four mutants were very similar to the wild-type protein. The high similarity between wild-type and mutant protein spectra indicated similar percentages of secondary structure elements between proteins.

A fluorescence-based thermal shift assay was subsequently used to determine the thermal stability of the mutants as compared to wild-type *Pa*FabA to investigate if the mutations had an impact on overall protein stability. These assays also provided useful information as to buffers suitable for crystallization.

For every sample experiments were performed in triplicate and the averages were taken. Our control buffer was the one used in all purification experiments (10 mM Tris pH 7.5 and 150 mM NaCl (buffer B)) to compare the stability of the wild-type and the mutants (Figure 20).

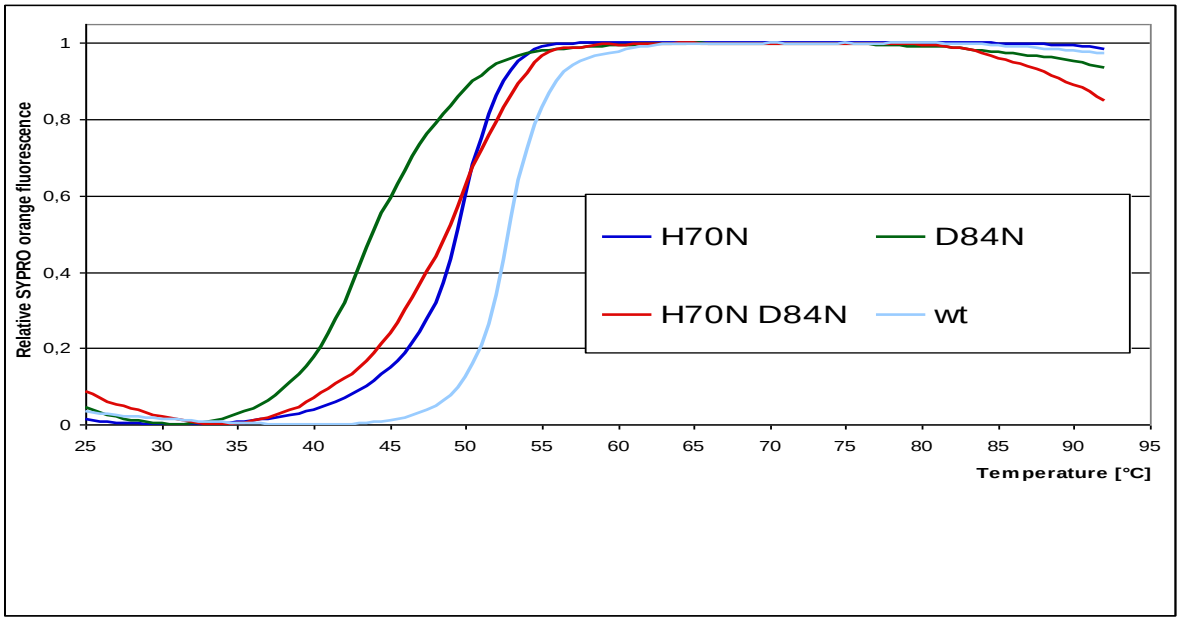

Figure 20: Thermal shift assay results for mutant and wild-type *Pa*FabA in Tris-buffer.
The melting curve of all four proteins was recorded as described in section 2.2.6. The wild-type *Pa*FabA (wt) shows the highest stability. Mutant D84N is less stable than mutants H70N/D84N and H70N.

With a melting temperature (T_m) of 52.8 ºC, the wild-type protein is more stable than the mutants. The mutants H70N (T_m = 49.3 ºC) and H70N/D84N (T_m = 48.6 ºC) show similar levels of stability while D84N (T_m = 44.1 ºC) shows the lowest melting temperature. Mutant H70Q was not used for these experiments because samples containing this protein always showed maximum fluorescence, even at room temperature.
This ranking of thermal stability (D84N < H70N/D84N ≈ H70N < wt) held true for all buffers tested as can be seen in Table 3.

Table 3: Melting temperatures of *Pa*FabA wild-type (wt) and mutant proteins in a range of buffers shown in ºC.

Buffer	wt	H70N	D84N	H70N/D84N
10 mM Tris pH 7.5 (A)	52.4	49.1	41.5	47.6
10 mM Tris pH 7.5; 150 mM NaCl (B)	52.8	49.3	44.1	48.6
10 mM Tris pH 7.5; 150 mM NaCl; 10 % glycerol (C)	54.5	51.7	44.9	49.4
10 mM Tris pH 7.5; 150 mM NaCl; 5 mM DTT (D)	53.1	49.7	44.1	49.0
50 mM sodium phosphate; 150 mM NaF (E)	57.0	53.2	47.8	52.0
10 mM Tris pH 7.5; 150 mM NaCl; 3-OH-decanoyl-NAC (F)	53.3	50.4	45.2	48.4
10 mM Tris pH 7.5; 150 mM NaCl; (E)-2-decanoyl-NAC (G)	52.7	50.0	45.8	48.7

The buffer with the most stabilizing effect contained sodium phosphate and sodium fluoride (buffer E), which was the buffer used to record the CD spectra. We tested several buffer conditions to detect influences of additives to our standard purification buffer (B) (glycerol or DTT) on protein stability and compared the mutants to the wild-type. Mutant H70N shows a small effect on the melting temperature when we added 10 % glycerol (+ 2.4 ºC), but no significant shift for the addition of 5 mM DTT (+ 0.4 ºC) or the absence of sodium chloride (- 0.2 ºC). The H70N mutant was most stable in phosphate buffer E (+ 3.9 ºC). The same trend is true for the wild-type protein. Mutant D84N is less stable in buffer A (- 2.6 ºC) and show no significant difference, when glycerol is added (+ 0.8 ºC). No significant shift was detected for the addition of 5 mM DTT. These experiments illustrate that the mutants behave like the wild-type protein across multiple buffer conditions, albeit at a slightly

lower melting temperature, and that the enzymes are folded under these different buffer conditions. Experiments with buffers F and G were surprising. The expectation was that both substrate analogs would stabilize the protein. However, 3-hydroxydecanoyl-NAC and (E)-decenoyl-NAC had no effect on the melting temperature.

In order to define the activity of the wild-type protein and the mutants, activity assays were performed using UV spectrophotometry. First, the substrate analogs 3-hydroxydecanoyl-N-acetylcysteamine (NAC) and (E)-2-decenoyl-NAC were synthesized by Dr. L. Moynie.

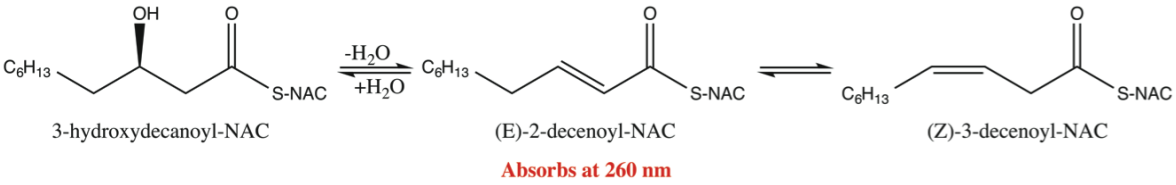

Figure 21: Reaction of the synthesized substrate mimics catalyzed by *Pa*FabA. (E)-2-decenoyl-NAC is the only UV active compound of the reaction and absorbs at 260 nm.

Based on the thermal shift assays, these experiments were performed in phosphate buffer (buffer E) to increase the stability of the protein. Only (E)-2-decenoyl-NAC absorbs at 260 nm, because of the conjugation between the (E)-2 carbon-carbon and the carbonyl double bonds. The conversion of 3-hydroxydecanoyl-NAC into (E)-2-decenoyl-NAC can therefore easily be measured by an increase in UV absorption. Similarly, the conversion of (E)-2-decenoyl-NAC into the other two compounds can be measured by a decrease in UV absorbance at 260 nm.

First, we added 0.3 mM (final concentration) of 3-hydroxydecanoyl-NAC to 14 µg of each protein (1.6 µM final concentration) giving a ~19-fold excess of substrate (Figure 22). As expected, wild-type *Pa*FabA shows rapid conversion of 3-hydroxydecanoyl-NAC into (E)-2-decenoyl-NAC. Mutants H70N, D84N, and H70N/D84N showed no activity. To our great surprise, *Pa*FabAH70Q showed residual activity. We therefore repeated the experiment with increased protein concentration and reaction speed was increased as well.

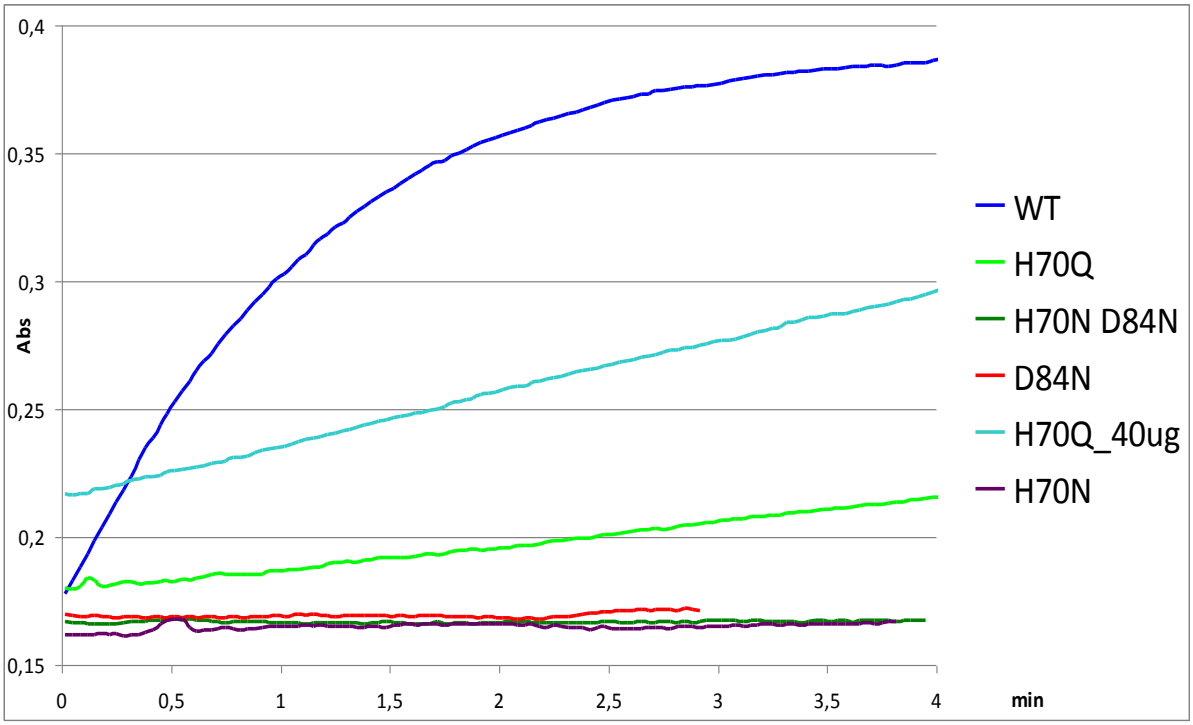

Figure 22: Enzymatic turnover of 0.3 mM 3-OH-decanoyl-NAC incubated with *Pa*FabA wild-type and mutant proteins. After addition of the substrate to enzyme and mutants the UV absorbance was recorded over several minutes. An increase in UV absorbance is attributed to the generation of (E)-2-decenoyl-NAC. Incubation with wild-type *Pa*FabA shows rapid conversion of 3-hydroxydecanoyl-NAC into (E)-2-decenoyl-NAC. Mutants H70N, D84N, and H70N/D84N showed no activity. H70Q showed residual activity and repeating the experiment with increased protein concentration speeded up the reaction.

Subsequently, we used 0.1 mM (E)-2-decenoyl-NAC in the same experimental set-up to ensure that the mutants were inactive for the production of (Z)-3-decenoyl-NAC as well, and that the mutations did not merely disrupt the transition of 3-hydroxydecanoyl-NAC to (E)-2-decenoyl-NAC (Figure 23). Again, the wild-type enzyme shows rapid conversion of 3-hydroxydecanoyl-NAC, which was measured as a decrease in the UV absorbance. The mutants H70N, D84N, and H70N/D84N are completely inactive. *Pa*FabAH70Q does again show residual activity.

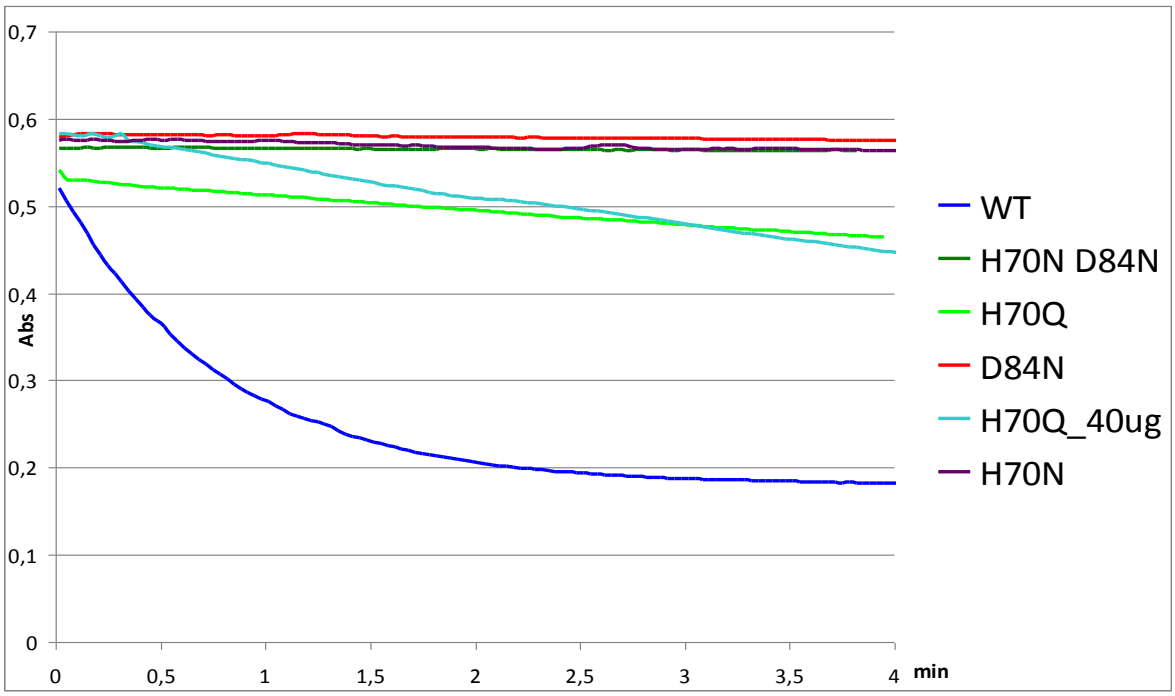

Figure 23: Enzymatic turnover of 0.1mM (E)-2-decenoyl-NAC with *Pa*FabA wild-type and mutant proteins. After addition of the substrate to enzyme and mutants the UV absorbance was recorded over several minutes. A decrease in UV absorbance is attributed to the conversion of (E)-2-decenoyl-NAC. The wild-type enzyme shows rapid conversion of 3-hydroxydecanoyl-NAC, which was measured as a decrease in the UV absorbance. The mutants H70N, D84N, and H70N/D84N are completely inactive. Mutant H70Q does again show residual activity.

3.3 Crystallization of mutants H70Q, H70N, D84N and H70N/D84N

To understand the mode of substrate binding of *Pa*FabA as well as the catalytic mechanism, we sought to determine the crystal structures of one of our mutants in the apo and substrate-bound forms. We performed crystal screening experiments for all mutants at a protein concentration of 6 mg/mL. Although we screened through >1000 stochastic conditions per mutant, no crystals could be obtained for the mutants H70Q, D84N and H70N/D84N. Initial crystals were found for *Pa*FabAH70N and were further optimized in hanging drop experiments (2 µl protein /1 µl mother liquid) with 25 % PEG 4000, 0.1 M sodium citrate pH 5 and 0.05 M ammonium sulfate at 20 °C (Figure 24).

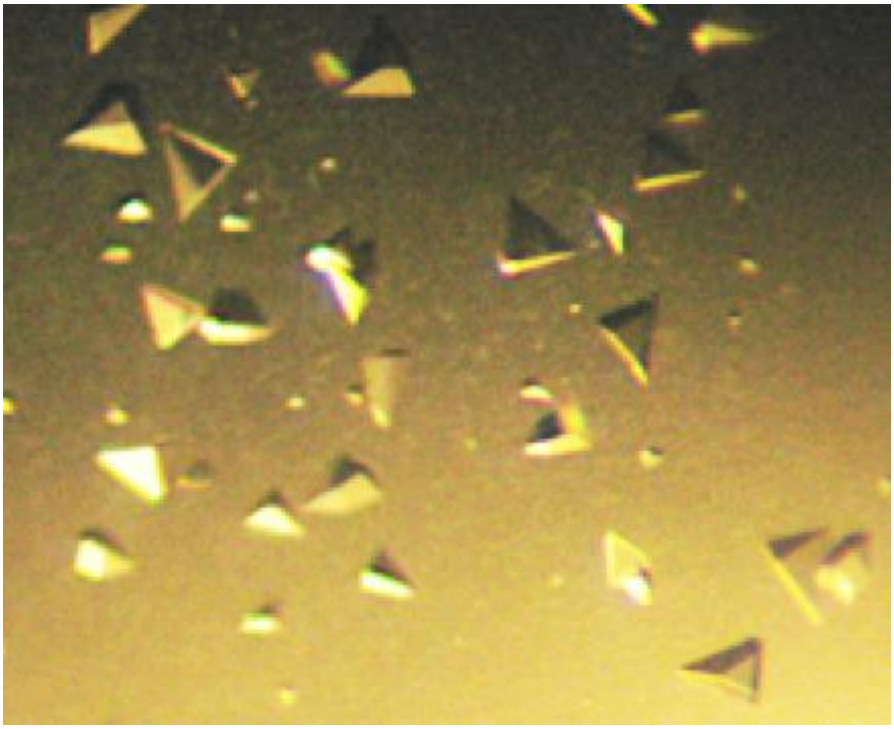

Figure 24: Crystals of *Pa*FabAH70N. Crystals were detected in 25 % PEG 4000, 0.1 M sodium citrate pH 5 and 0.05 M ammonium sulfate at 20 °C.

The crystals were cryoprotected in mother liquor containing 15 % glycerol and flash-frozen in liquid nitrogen. The structure of *Pa*FabAH70N was determined to 2.1 Å resolution by molecular replacement using our *Pa*FabA wild-type structure as a search model (Figure 25). Data collection and refinement statistics are shown in Table 4.

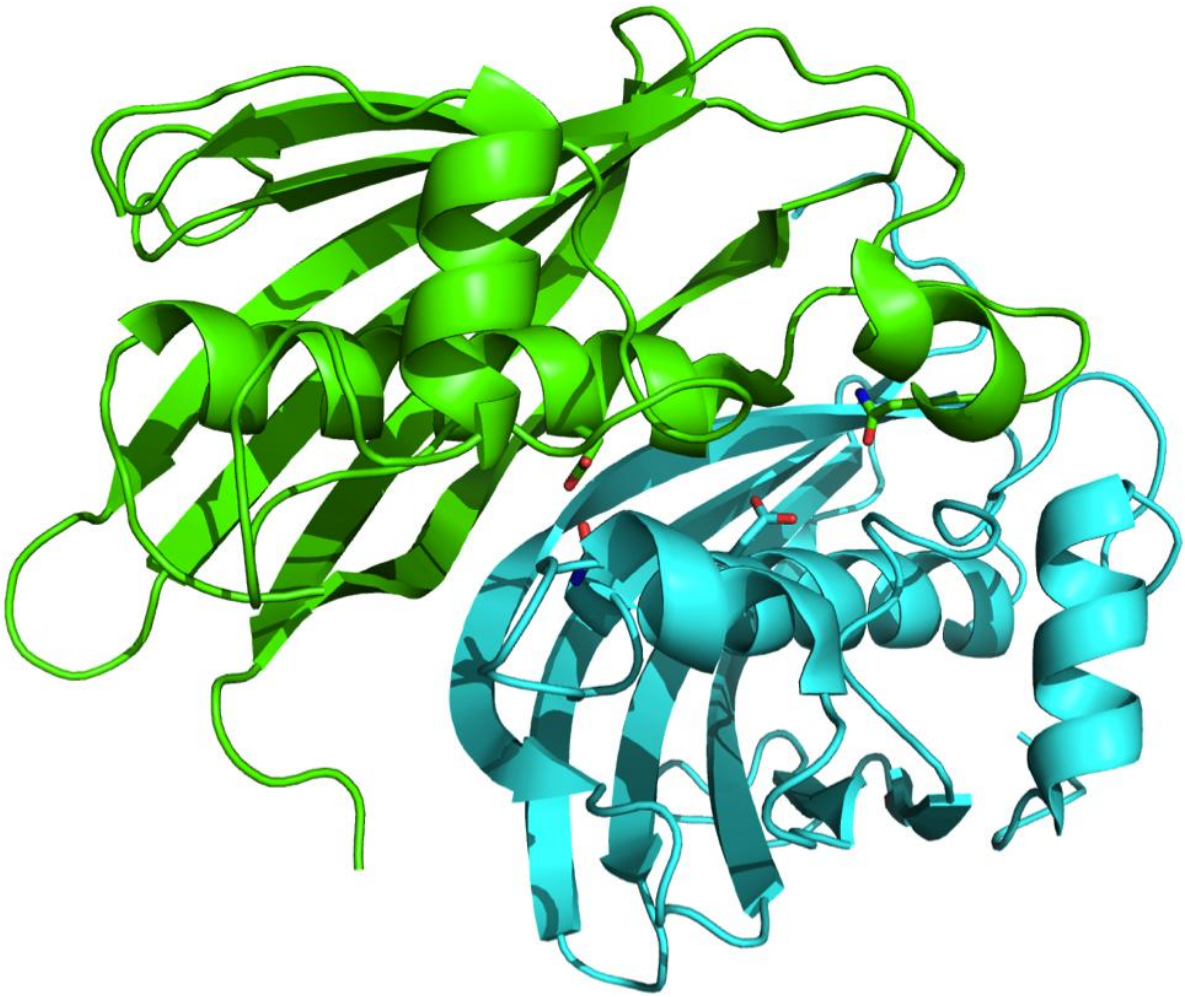

Figure 25: Cartoon representation of the overall structure of *Pa*FabAH70N. Dimerization is essential for activity since the active site is comprised of residues from both dimer partners. The structure was determined at a resolution of 2.1 Å. Catalytic residues shown as sticks (N70 and D84).

Table 4: Data collection and refinement statistics for the structures of PaFabAH70N in the substrate bound and unbound forms. Statistics for the highest resolution shell are shown in parentheses.

	H70N	H70N with 3-OH-decanoyl-NAC
Space group	C2	$C222_1$
a, b, c (Å)	114.9, 142.3, 78.1	110.8, 169.7, 108.3
α, β, γ (°)	90.0, 116.5, 90.0	90.0 ,90.0 ,90.0
Resolution (Å)	60-2.1 (2.23-2.1)	50-2.13 (2.15-2.03)
R_{sym} (%)	5.8 (52.0)	5.8 (46.0)
Completeness (%)	97 (93.3)	97.6 (96.9)
I/σI	15.8 (2.7)	15.4 (2.5)
R/R_{free}	0.21/0.23	0.19/0.22

The final model of *Pa*FabAH70N is fully ordered and each monomer consists of a long curved six-stranded antiparallel β-sheet flanked by two perpendicular α-helices. The structure of *Pa*FabAH70N is virtually identical to the wild-type structure. Pairwise superposition with *Pa*FabA gave an rmsd of 0.58 Å for 166 Cα positions. As with the wild-type protein and in agreement with the gel filtration results, *Pa*FabAH70N forms dimers within the crystal. The dimer has an ellipsoidal shape with dimensions of approximately 115 Å × 142 Å × 78 Å and the crystal lattice contains pentameric ring of dimers, with two and a half dimers in the asymmetric unit (Figure 26). The strong dimer interface consists of an intricate network of 20 hydrogen bonds and 10 salt-bridges, as well as many hydrophobic interactions which overall involve 44 residues per monomer (See Appendix 1). The active site of *Pa*FabAH70N contains the putative catalytic residues H70, mutated to N, and D84.

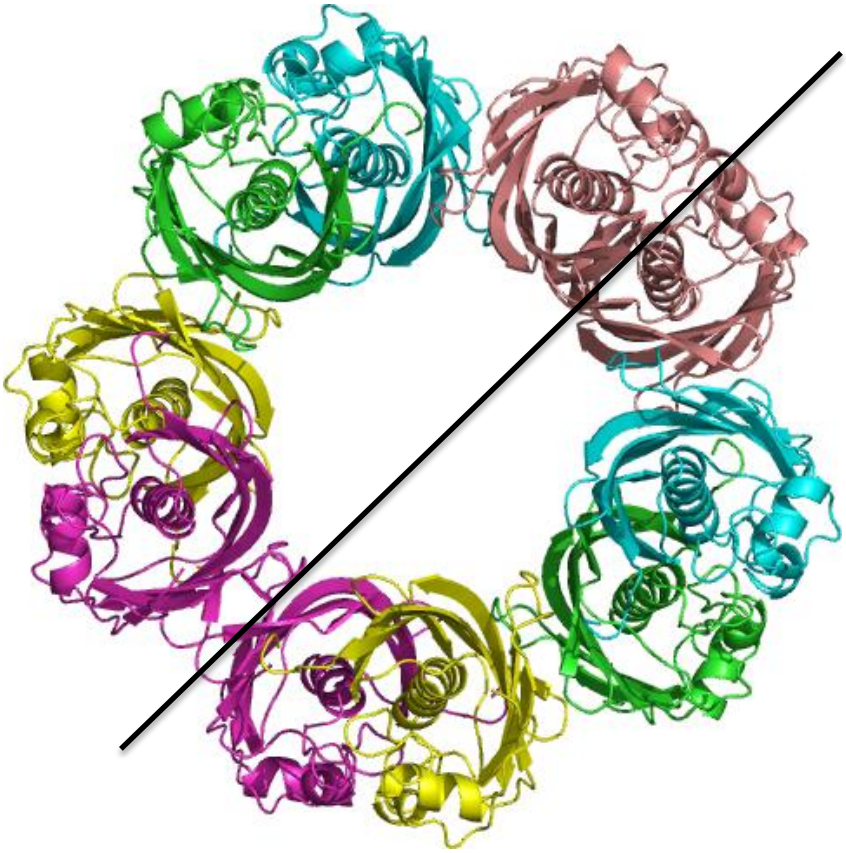

Figure 26: Packing within the *Pa*FabAH70N crystal lattice showing the biological hexamer in two asymmetric units. The two-fold symmetry axis is shown as a black line.

The next goal was to crystallize the complex of *Pa*FabAH70N with 3-hydroxyl-decanoyl-NAC or (E)-2-decenoyl-NAC. The H70N crystals were very fragile and not amenable to soaking. Therefore co-crystallization was attempted and the enzyme at 7 mg/mL was incubated with 1 mM 3-hydroxy-decanoyl-NAC for 2 h on ice before setting up crystallization plates for grid-screens around the condition that yielded diffraction quality crystals of the apo-protein. We were unable to reproduce H70N crystals in the presence of the compound in this crystallization condition and therefore opted for stochastic screening of a large number of conditions. Initial hits were optimized in hanging drops in 11 % PEG 5K MME, 80 mM lithium sulfate and 0.1 M sodium citrate pH 4.5 (2 µl protein /1 µl mother liquor) at 20 °C (Figure 27).

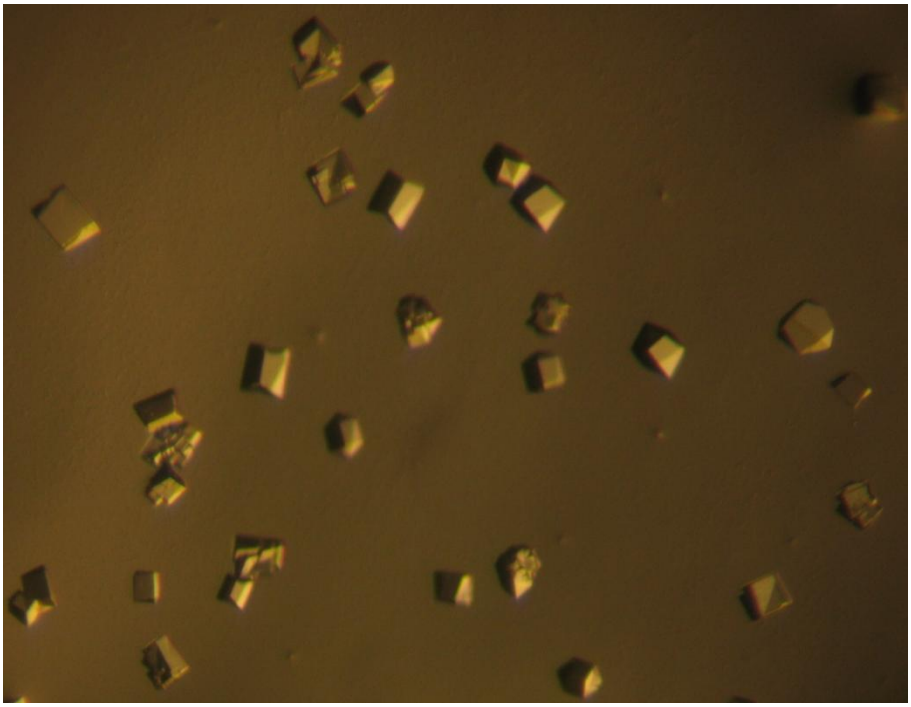

Figure 27: Crystals of *Pa*FabAH70N in complex with 3-hydroxy-decanoyl-NAC. They were detected in 11 % PEG 5K MME, 80 mM lithium sulfate and 0.1 M sodium citrate pH 4.5 (2 µl protein /1 µl mother liquor) at 20 °C.

Data for *Pa*FabAH70N/3-hydroxydecanoyl-NAC was collected at ESRF ID-29 to 2.0 Å and solved by molecular replacement with PHASER, using wild-type coordinates as the search model. The model and structure factors have been deposited in the Protein Data Bank under the code 4B0I. Data collection and refinement statistics are shown in Table 4.

There are five monomers in the asymmetric unit, which are highly similar except for the very C-terminal residues. The protomer used for the description of the structure is the best-ordered chain D and its dimer partner chain C. There are no large structural rearrangements as a result of substrate binding which is reflected by an rmsd of 0.58 Å for 166 Cα positions between the apo and substrate-bound structures. The differences between the six C-terminal residues of the two structures are a result of crystal packing with the exception of F171, which adopts a distinct rotamer due to contacts with the bound substrate.

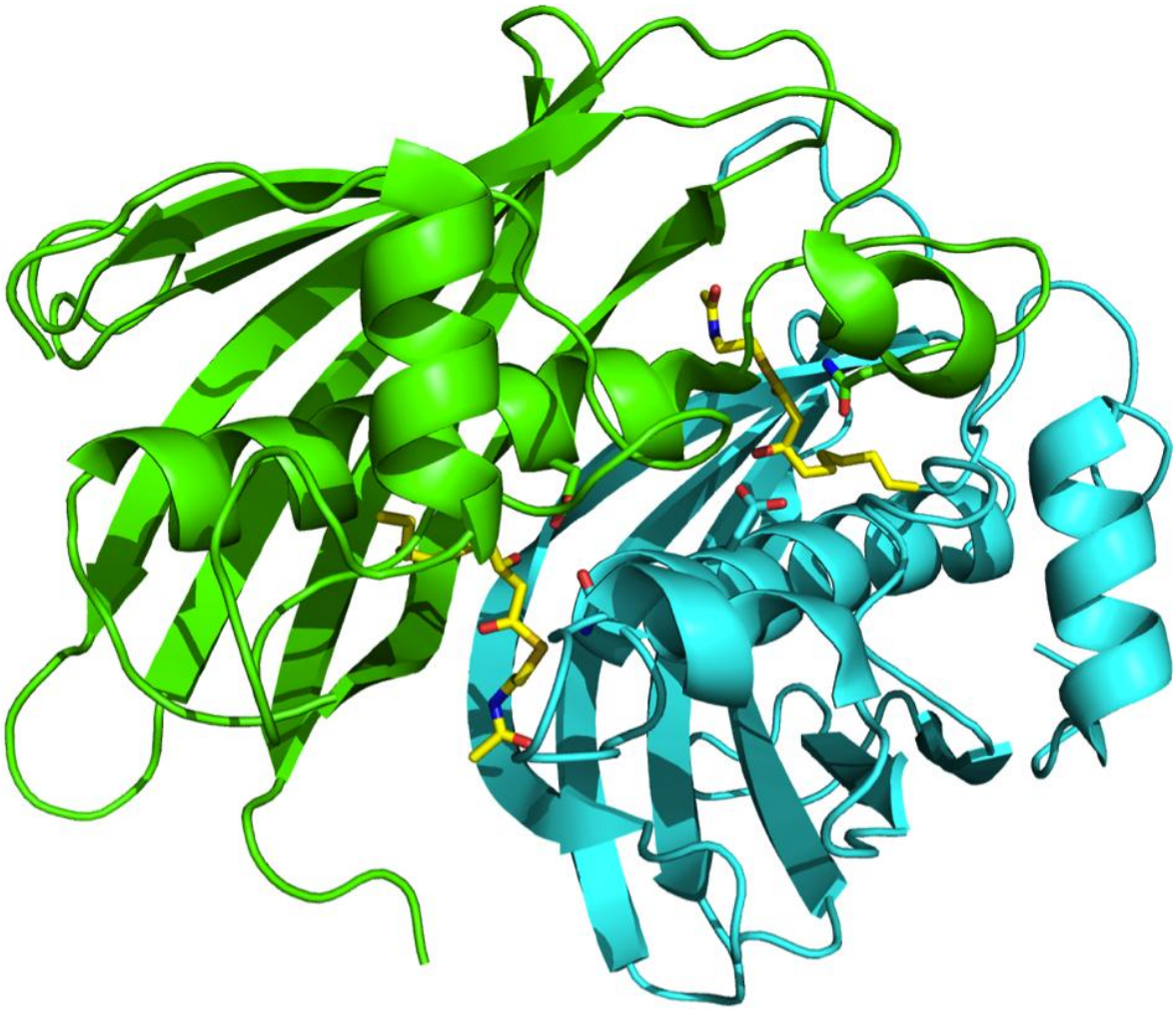

Figure 28: Overall structure of *Pa*FabAH70N dimer with 3-hydroxydecanoyl-NAC in the active site. The catalytic residues H70 and D84 and 3-hydroxydecanoyl-NAC are shown as sticks.

The substrate is bound by both proteins across the dimer interface (Figure 28). The N-acetylcysteamine moiety of the substrate is bound in a tunnel formed by β3 of one monomer and the α2-α3 and β3-β4 loops of the other. In addition to hydrophobic contacts this region of the substrate also forms two hydrogen bonds (Figure 29).

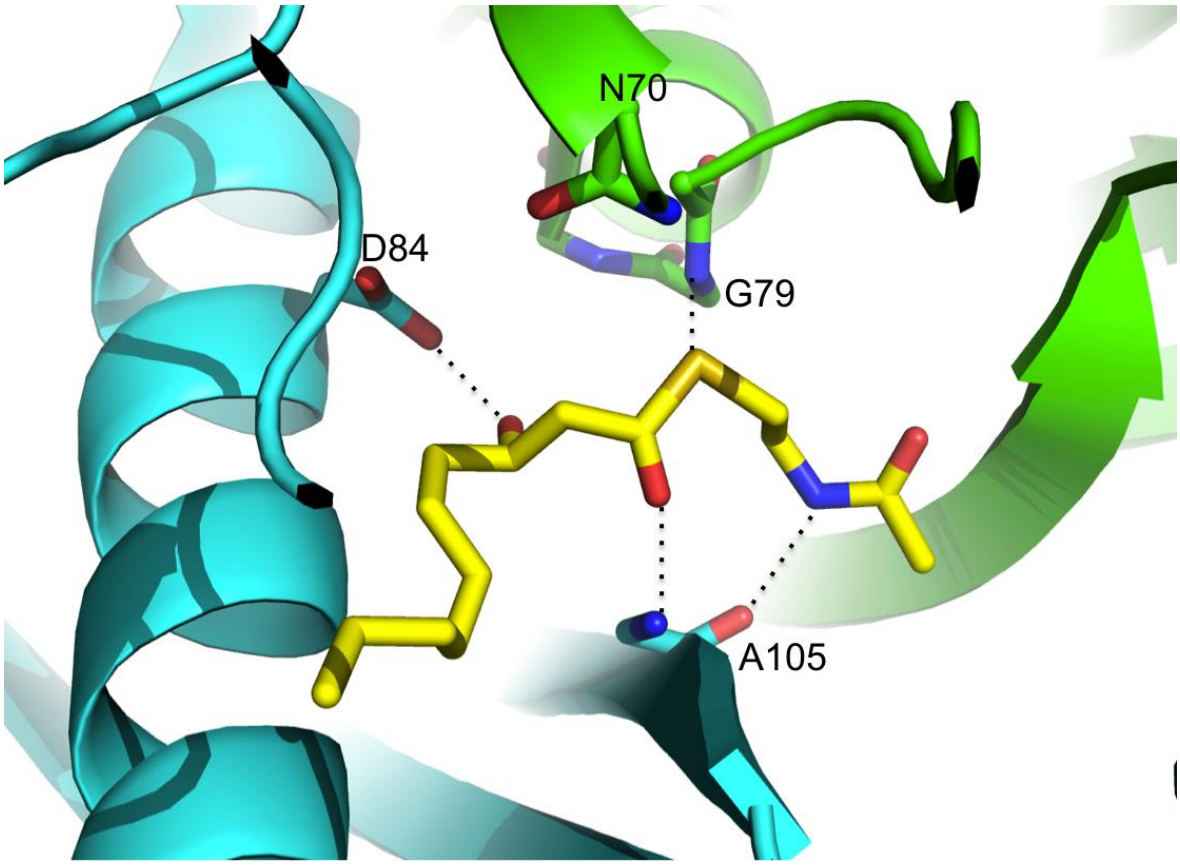

Figure 29: Hydrogen bonds formed between the *Pa*FabAH70N dimer and 3-hydroxydecanoyl-NAC. Hydrogen bonds are shown as dashed lines, 3-hydroxydecanoyl-NAC as yellow and interacting (and catalytic) protein residues as green/cyan sticks, oxygen atoms in red and nitrogen atoms in blue.

In the N-acetylcysteamine part of the substrate two hydrogen bonds are formed, one between the substrate's NH and the carbonyl group of A105, while the second is formed between the carbonyl and a well ordered water molecule, which itself makes a network of hydrogen bonds including to the hydroxyl of Y155, the carbonyl of M77 and the amine of V117.

The lipidic part of 3-hydroxydecanoyl-NAC also forms hydrogen bonds with the protein. The lipid carbonyl forms a hydrogen bond with the amide of A105 while the 3-hydroxy group makes two hydrogen bonds, one with the side chain carboxy group of D84 and a second with another well-ordered water molecule (W1), which is itself coordinated by the carbonyl of D84, amine of C80 and amine of G79. The aliphatic chain of 3-hydroxydecanoyl-NAC is embedded in a hydrophobic tunnel formed by α3, β3 and α1-β1 loop and virtually completely

protected from bulk solvent (Figure 30). C4-10 of the lipid lie parallel to α3 and exhibit van der Waals interactions with residues of the end of the active site: Q27, P78, Q88, G91, G103, V162. The amine of the side chain of N70 makes the same hydrogen bond to the carbonyl of V76 as Nδ1 of H70 in the wild-type. F71 and P78, which stack against the imidazole ring, are unchanged.

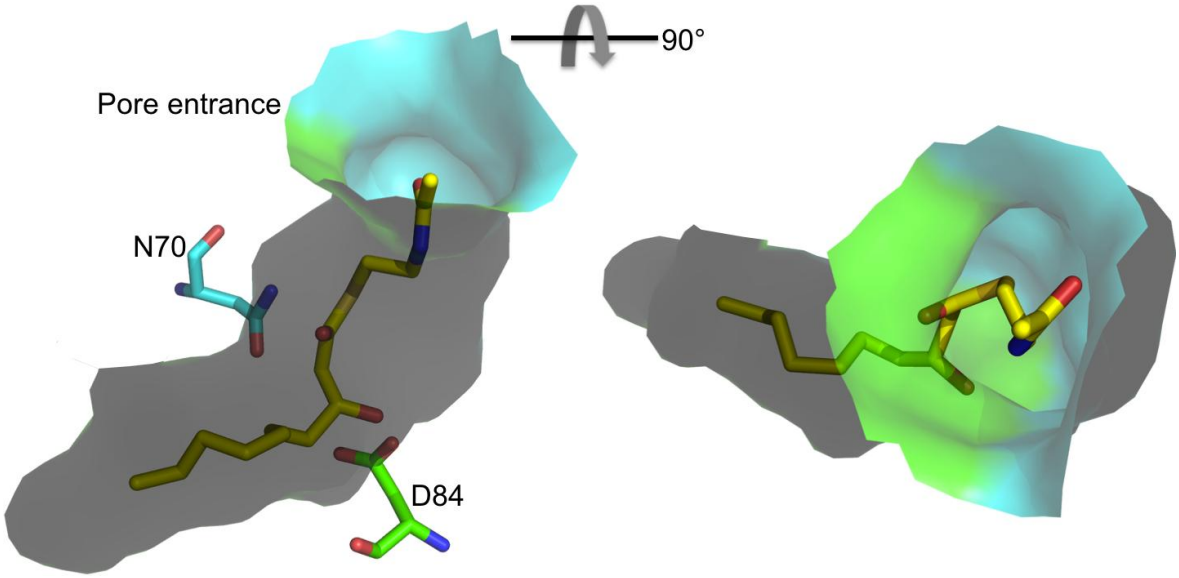

Figure 30: Hydrophobic substrate binding pocket. The very deep substrate binding pocket is created by the dimer molecules A and B (green and cyan) at the dimer interface. Substrate and catalytic residues are shown as sticks with one catalytic residue contributed from each monomer.

Comparing this complex structure with the *Ec*FabA/3-decenoyl-NAC complex (PDB 1MKA) shows several key differences between the two structures. The enzymes are very similar (Cα rmsd of 0.63 Å for 166 residues) but crucially in the *Ec*FabA structure the substrate is covalently bound to the enzyme by a bond between the C3 of the substrate and the side chain of H70. The result is a shift of the NAC group further along the binding groove and away from the active site while the aliphatic tail is pulled in towards the active site, relative to the complex described here. As a consequence, the C1-4 atoms of the lipid are misaligned between the two structures and displaced by ~2 Å. The interactions

between the catalytic residues and the lipids are thus very different (see discussion).

Co-crystallization of the mutant H70N with (E)-2-decenoyl-NAC was attempted and data collected from optimized crystals. Unfortunately co-crystals could only be obtained in acidic conditions, which was sufficient to hydroxylate (E)-2-decenoyl-NAC to 3-hydroxydecanoy-NAC to form the complex for which we already obtained a structure and at a lower resolution.

4 DISCUSSION

The first goal of this work was to produce *Pa*FabA mutants, which would be inactive but still structurally virtually identical to the wild-type protein. The four mutatations selected (H70N, H70Q, D84N and H70N/D84N) were all very conservative. Generally, mutating these residues to alanines would have been effective from a catalytic point of view but might have distorted the structure and thus impeded the insights gained from possible structures of the mutant in complex with substrate. All four mutants were expressed under different conditions to the wild-type, but purified in the same way. Initial expression of all four mutants showed low expression levels and the majority of the expressed protein was insoluble. Since all experiments depended on soluble protein, the expression conditions (expression strains, temperatures, incubation times, media types and IPTG concentrations) were systematically varied to achieve good yields of soluble protein. The best method was the use of auto-induction medium, which contains a mixture of glucose, glycerol and lactose. Once all glucose is consumed, the *E. coli* metabolism switches to process lactose, activating the *lac* operon thus allowing the expression of T7 polymerase which causes expression of our proteins of interest which have T7 promotors. Lactose is a more potent inducer of expression than IPTG and generally results in significantly higher levels of overexpression. To ensure that the large amounts of target protein were soluble the expression temperature was reduced to 20 °C

to aid protein stability. The resulting yields of up to 105 mg purified, soluble protein per liter of culture were more than sufficient to perform all experiments described here.

All mutants were purified like the wild-type protein. SDS-PAGE analysis of samples from the second Ni-affinity purification step showed residual amounts of enzyme in the elution step indicating incomplete cleavage with TEV protease. The lost amounts of enzyme were insignificant compared to the digested amount of protein. The gel filtration elution profile of D48N showed that it eluted at the same elution volume as the wild-type enzyme while the profiles of H70Q, H70N, H70N/D84N were still very similar to the wild-type enzyme, indicating that the mutations had not disrupted the dimer interface. In such a case a dramatic shift in the elution volume would have been observed. Interestingly, all enzymes with a mutation at residue H70 showed slightly earlier elution volumes. Since the shift was within the experimental error of the column calibration runs, no change in the dimeric state of these mutants appeared to have occurred. This indicated a little shift to a larger apparent hydrodynamic radius or a small decrease in the interactions between the protein and the column resin. *Pa*FabA H70Q showed two peaks of equal size during gel filtration. The first peak eluted at a much higher apparent molecular weight which would correspond to aggregated *Pa*FabA. This was surprising since there was no indication this protein was aggregating until this final step. In hindsight the structure of wild-type *Pa*FabA offers an explanation. When H70 is mutated *in silico* to N all side-chain rotamers can be accommodated without clashes. In the H to Q mutation on the other hand the additional methylene group (compared to N) causes clashes in all side-chain rotamers, most notably with F71 and P78 as well as P29 and M33 of the dimer partner. Only the second peak of H70Q, corresponding to the dimer, was collected and used for further experiments. CD spectroscopy of all mutant enzymes showed very similar spectra compared to the wild-type protein, which demonstrates that the mutants were folded as expected from gel filtration.

Problems with *Pa*FabAH70Q continued during thermofluor analysis, where it was the only protein that gave no data. The measured fluorescence intensity

was always at maximum, even at room temperature. A possible explanation would be that the protein was already partly unfolded or contained significant amounts of aggregated protein, which binds to the dye and thus gives a false positive signal in the assay. Both explanations are at odds with the CD data, which showed folded protein. Since the second protein peak, which was collected, eluted like the other two H70 mutants in gel filtration and shows the same CD absorbance spectrum as the others, it might still be possible that at least a part of the protein in our sample aggregated.

The other mutants, H70N, D84N, H70N/D84N, which could be used in thermofluor experiments, all showed decreased stability compared to the wild-type as indicated by shifts to lower T_m values. In the most stabilizing buffer, H70N showed a small decrease in stability (- 3.8 °C) while D84N resulted in a dramatic shift of - 9.2 °C compared to wild-type. The double mutant was intermediate between the two single mutants at - 5 °C, which shows that the decrease in protein stability as a result of the mutations is not additive. Therefore the H70N mutation helps to stabilize the D84N mutation specifically and not D84 itself.

The large decrease in thermal stability of the mutants, especially for D84N, was surprising since the mutations were conservative and we knew from the wild-type structure that these two residues were not involved inter-dimer interactions. But since both residues, but most notably D84, are involved in intricate hydrogen-bonding networks in the active site (see results) the little changes seem to have effects on stability within the monomers. Additives to protein buffers such as DTT and glycerol can have stabilizing effects on proteins but in the case of *Pa*FabA the gains were within the experimental error of ~ 2 °C. Many high-throughput screens for new drug targets use thermofluor data under the assumption that a compound binding to the protein will increase its thermal stability. For *Pa*FabA there was no significant effect on protein stability by addition of the substrates 3-hydroxydecanoyl-NAC and (E)-decenoyl-NAC. This was unexpected since substrate binding similar to that of *Ec*FabA would involve many interactions between the enzyme and the substrate across both protomers of the dimer.

Thermofluor condition E (50 mM sodium phosphate; 150 mM NaF) was originally tested to ensure that the enzymes were stable in the buffer used for CD spectroscopy. While it proved to be the most stabilizing buffer, possibly due to phosphate binding in the active site, this buffer was not chosen for crystal screening. Phosphate and fluoride ions are notorious for forming salt crystals with divalent cations and thus give false positives in crystal screens. This prevents crystallization space with conditions containing divalent cations from being sampled efficiently.

The activity assays confirmed that three of the mutants (D84N, H70N and H70N/ D84N) were catalytically inactive. Only H70Q showed activity which was surprising given the thermofluor experiments, although CD suggested folded protein. The residual activity might be due to this mutation being too conservative. As can be seen in Figure 31, it is possible that the primary ε2 amino group of glutamine may compensate for the loss of the secondary ε2 amino group of histidine. If the thermofluor data is accurate the reaction of H70Q might progress if all the protein in the sample was still folded.

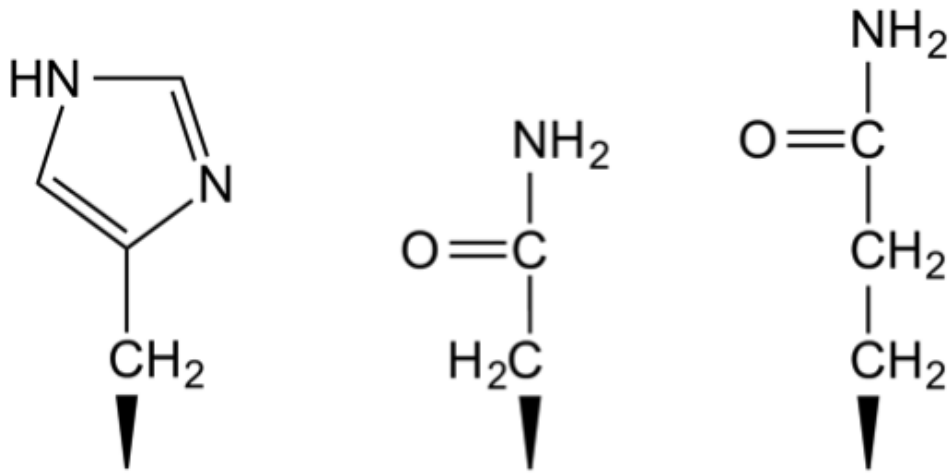

Figure 31: Chemical structure of amino acid side chains from histidine, asparagine and glutamine residues (left to right).

The substrate excess used in the activity experiments is not suitable to determine a turnover rate and the fact that the bifunctional enzyme produces three compounds, all of which are all in equilibrium, complicates interpretation of the data. Assuming an endpoint of the reaction is reached when the UV

absorbance in Figure 23 and Figure 24 plateaus, one estimate is that as much as 50 % of enzyme activity may be retained by *Pa*FabAH70Q. The mutation of H to N on the other hand places the asparagine δ2 amino group one full carbon-carbon bond-length away from the original position and prohibits even residual activity. The importance of the acidic nature of D84 is highlighted by the fact that the D84N mutation inactivates the enzyme.

The *Pa*FabAH70N complex structure with 3-hydroxydecanoyl-NAC allows insights into the enzymatic mechanism. For 3-hydroxydecanoyl-NAC to be converted into (E)-2-decenoyl-NAC the 3-hydroxyl must be eliminated. The simplest way this can occur is by removal of a proton from the C2 position followed by elimination of the protonated C3 hydroxyl group. H70 is in a perfect position to act as the general base while D84 from the other protomer forms a hydrogen bond to the hydroxyl group and so may act as the general acid. While most aspartic acid residues are deprotonated at physiological pH, the immediate surroundings of any amino acid can shift the pKa significantly. This can be due to hydrogen bonding networks, the presence of additional charged amino acids or a hydrophobic environment. In the case of *Pa*FabA D84 is located in a largely hydrophobic active site and also forms hydrogen bonds to other residues, making a protonated D84 likely. It is important to note that a structured water molecule is found in both the H70N apo and complex structures. It has previously been suggested that this water molecule is a product of the elimination reaction (Kimber et al. 2004), but its presence in the complex of enzyme with substrate rather than product makes this very unlikely. This water also forms extensive hydrogen bonds with enzyme and substrate, which suggests that it may play a catalytic role in the reaction, perhaps as a proton relay between D84 and the substrate's hydroxyl.

The second reaction catalyzed by FabA is the conversion of (E)-2-decenoyl-NAC to (Z)-3-decenoyl-NAC. The isomerization reaction requires deprotonation at C4 and reprotonation at C2. D84, which was deprotonated in the first reaction, is the most likely candidate as the base. The D84 carboxyl is only 4.1 Å away from C4 and therefore only a small movement of C4 would be needed. We cannot speculate on the identity of the acid.

The enzymes of FAS II in Gram-negative organisms remain interesting targets for the development of antibacterial drugs (Campbell and Cronan 2001). The substrate complex *Pa*FabAH70N/3-hydroxydecanoyl-NAC clarifies the mechanistic details of the active site. After finishing this work, the stucture of FabA in complex with four binding fragments was discovered which occupy different positions in the active site. These fragments serve as the first step for a rational inhibitor design program (Moynie et al. 2013).

5 SUMMARY

Pseudomonas aeruginosa is an important Gram-negative bacterial pathogen that causes a broad spectrum of infections in humans. It is a particular threat in ICUs, where *P. aeruginosa* has become a leading cause of nosocomial infections in immuno-compromised and debilitated patients. Infections may be linked with great morbidity and mortality and their treatment has become difficult due to the increasing frequency of multi-drug-resistant strains and a shortage of new antibiotics.

In *P. aeruginosa* the protein FabA, a β-hydroxydecanoyl thioester dehydrase, is essential for the biosynthesis of unsaturated fatty acids and thus of bacterial cell membranes. FabA catalyzes the dehydration of (R)-3-hydroxydecanoyl-acyl carrier protein to (E)-2-decenoyl-acyl carrier protein and the isomerization to (Z)-decenoyl-acyl carrier protein. The importance of fatty acids in the organism and the lack of human homologs make *Pa*FabA a potential target for new antibiotics.

The aim of the work was to elucidate the function and mechanism of the enzyme *Pa*FabA through structural and biochemical characterizations. We expressed, purified and crystallized *Pa*FabAH70N in the presence and absence of a substrate analog. This mutant and a further three mutants were characterized biochemically (UV spectrometry activity assays) and biophysically (fluorescence-based thermal shift assays). The biochemical data supported the mechanism proposed on the basis of the structural data.

6 REFERENCES

Aguilar PS, Cronan JE Jr., de Mendoza D (1998) A Bacillus subtilis Gene Induced by Cold Shock Encodes a Membrane Phospholipid Desaturase. Bacteriol. 180(8): 2194–2200.

Akasaka T, Tanaka M, Yamaguchi A, Sato K (2001) Type II topoisomerase mutations in fluoroquinolone-resistant clinical strains of Pseudomonas aeruginosa isolated in 1998 and 1999: role of target enzyme in mechanism of fluoroquinolone resistance. Antimicrob Agents Chemother 45(8): 2263-8.

Anderson AC (2003) The process of structure-based drug design. Chem Biol 10(9): 787-97.

Aquino VM, Pappo A, Buchanan GR, Tkaczewski I, Mustafa MM (1995) The changing epidemiology of bacteremia in neutropenic children with cancer. Pediatr Infect Dis J 14(2): 140-3.

Avison MB (2005) New approaches to combating antimicrobial drug resistance. Genome Biol 6(13): 243.

Bal AM, Kumar A, Gould IM (2010) Antibiotic heterogeneity: from concept to practice. Ann N Y Acad Sci 1213: 81-91.

Baldock C, Rafferty JB, Stuitje AR, Slabas AR, Rice DW (1998) The X-ray structure of Escherichia coli enoyl reductase with bound NAD+ at 2.1 A resolution. J Mol Biol 284(5): 1529-46.

Banerjee A, Dubnau E, Quemard A, Balasubramanian V, Um KS, Wilson T, Collins D, de Lisle G, Jacobs WR Jr. (1994) inhA, a gene encoding a target for isoniazid and ethionamide in Mycobacterium tuberculosis. Science 263(5144): 227-30.

Bassetti M, Righi E, Viscoli C (2008) Pseudomonas aeruginosa serious infections: mono or combination antimicrobial therapy? Curr Med Chem 15(5): 517-22.

Bennett KM, Scarborough JE, Sharpe M, Dodds-Ashley E, Kaye KS, Hayward TZ 3rd, Vaslef SN (2007) Implementation of antibiotic rotation protocol improves antibiotic susceptibility profile in a surgical intensive care unit. J Trauma 63(2): 307-11.

Berka RM, Vasil ML (1982) Phospholipase C (heat-labile hemolysin) of Pseudomonas aeruginosa: purification and preliminary characterization. J Bacteriol 152(1): 239-45.

Bottone EJ, Perez AA 2nd (1993) Pseudomonas aeruginosa folliculitis acquired through use of a contaminated loofah sponge: an unrecognized potential public health problem. J Clin Microbiol 31(3): 480-3.

Bryan LE, O'Hara K, Wong S (1984) Lipopolysaccharide changes in impermeability-type aminoglycoside resistance in Pseudomonas aeruginosa. Antimicrob Agents Chemother 26(2): 250-5.

Burgess DS, Hastings RW (2000) Activity of piperacillin/tazobactam in combination with amikacin, ciprofloxacin, and trovafloxacin against Pseudomonas aeruginosa by time-kill. Diagn Microbiol Infect Dis 38(1): 37-41.

Burns JL, Ramsey BW, Smith AL (1993) Clinical manifestations and treatment of pulmonary infections in cystic fibrosis. Adv Pediatr Infect Dis 8: 53-66.

Campbell JW, Cronan JE Jr. (2001) Bacterial fatty acid biosynthesis: targets for antibacterial drug discovery. Annu. Rev. Microbiol. 55: 305-332.

Carlet J, Ben Ali A, Chalfine A (2004) Epidemiology and control of antibiotic resistance in the intensive care unit. Curr Opin Infect Dis 17(4): 309-16.

Carmeli Y, Troillet N, Eliopoulos GM, Samore MH (1999) Emergence of antibiotic-resistant Pseudomonas aeruginosa: comparison of risks associated with different antipseudomonal agents. Antimicrob Agents Chemother 43(6): 1379-82.

Clark DP, DeMendoza D, Polacco ML, Cronan JE Jr. (1983) Beta-hydroxydecanoyl thio ester dehydrase does not catalyze a rate-limiting step in Escherichia coli unsaturated fatty acid synthesis. Biochemistry 22(25): 5897-902.

Costerton JW, Stewart PS, Greenberg EP (1999) Bacterial biofilms: a common cause of persistent infections. Science 284(5418): 1318-22.

Cronan JE (2003) Bacterial membrane lipids: where do we stand? Annu Rev Microbiol 57: 203-24.

Cronan JE Jr., Li WB, Coleman R, Narasimhan M, de Mendoza D, Schwab JM (1988) Derived amino acid sequence and identification of active site residues of Escherichia coli beta-hydroxydecanoyl thioester dehydrase. J Biol Chem 263(10): 4641-6.

D'Agnolo G, Rosenfeld IS, Vagelos PR (1975) Multiple forms of beta-ketoacyl-acyl carrier protein synthetase in Escherichia coli. J Biol Chem 250(14): 5289-94.

Dalhoff A, Janjic N, Echols R (2006) Redefining penems. Biochem Pharmacol 71(7): 1085-95.

Davies JC (2002) Pseudomonas aeruginosa in cystic fibrosis: pathogenesis and persistence. Paediatr Respir Rev 3(2): 128-34.

Davis AM, Teague SJ, Kleywegt GJ (2003) Application and limitations of X-ray crystallographic data in structure-based ligand and drug design. Angew Chem Int Ed Engl 42(24): 2718-36.

De Mendoza D, Klages UA, Cronan JE Jr. (1983) Thermal regulation of membrane fluidity in Escherichia coli. Effects of overproduction of beta-ketoacyl-acyl carrier protein synthase I. J Biol Chem. 258(4):2098-101.

Doig P, Todd T, Sastry PA, Lee KK, Hodges RS, Paranchych W, Irvin RT (1988) Role of pili in adhesion of Pseudomonas aeruginosa to human respiratory epithelial cells. Infect Immun 56(6): 1641-6.

Donlan RM (2002) Biofilms: microbial life on surfaces. Emerg Infect Dis 8(9): 881-90.

Doring G, Conway SP, Heijerman HG, Hodson ME, Høiby N, Smyth A, Touw DJ (2000) Antibiotic therapy against Pseudomonas aeruginosa in cystic fibrosis: a European consensus. Eur Respir J 16(4): 749-67.

Emori TG, Gaynes RP (1993) An overview of nosocomial infections, including the role of the microbiology laboratory. Clin Microbiol Rev 6(4): 428-42.

Encyclopedia Britannica (2009)

Evans P (2006) Scaling and assessment of data quality. Acta Crystallogr D Biol Crystallogr 62(Pt 1): 72-82.

FEDESA (1998) Animal Health. Dossier 15 zit. In Deut. Tierärzteblatt 46, 1093

Fernandes P (2006) Antibacterial discovery and development-the failure of success? Nat Biotechnol 24(12): 1497-503.

Filiatrault MJ, Picardo KF, Ngai H, Passador L, Iglewski BH (2006) Identification of Pseudomonas aeruginosa genes involved in virulence and anaerobic growth. Infect Immun 74(7): 4237-45.

Fischbach MA, Walsh CT (2009) Antibiotics for emerging pathogens. Science 325(5944): 1089-93.

Fisher MC, Goldsmith JF, Gilligan PH (1985) Sneakers as a source of Pseudomonas aeruginosa in children with osteomyelitis following puncture wounds. J Pediatr 106(4): 607-9.

Fishman JA, Rubin RH (1998) Infection in organ-transplant recipients. N Engl J Med 338(24): 1741-51.

Fleming A (1929) On the Antibacterial Action of Cultures of a Penicillium, with Special Reference to their Use in the Isolation of B. influenzæ. Br J Exp Pathol. 10(3): 226–236.

Freiberg C, Brunner NA, Schiffer G, Lampe T, Pohlmann J, Brands M, Raabe M, Häbich D, Ziegelbauer K (2004) Identification and characterization of the first class of potent bacterial acetyl-CoA carboxylase inhibitors with antibacterial activity. J Biol Chem 279(25): 26066-73.

Furuya EY, Lowy FD (2006) Antimicrobial-resistant bacteria in the community setting. Nat Rev Microbiol 4(1): 36-45.

Gales AC, Jones RN, Turnidge J, Rennie R, Ramphal R (2001a) Characterization of Pseudomonas aeruginosa isolates: occurrence rates, antimicrobial susceptibility patterns, and molecular typing in the global SENTRY Antimicrobial Surveillance Program, 1997-1999. Clin Infect Dis 32 Suppl 2: S146-55.

Gales AC, Reis AO, Jones RN (2001b) Contemporary assessment of antimicrobial susceptibility testing methods for polymyxin B and colistin: review of available interpretative criteria and quality control guidelines. J Clin Microbiol 39(1): 183-90.

Garwin JL, Klages AL, Cronan JE Jr. (1980) Structural, enzymatic, and genetic studies of beta-ketoacyl-acyl carrier protein synthases I and II of Escherichia coli. J Biol Chem 255(24): 11949-56.

Gelmann EP, Cronan JE Jr. (1972) Mutant of Escherichia coli deficient in the synthesis of cis-vaccenic acid. J Bacteriol 112(1): 381-7.

Giamarellou H (2002) Prescribing guidelines for severe Pseudomonas infections. J Antimicrob Chemother 49(2): 229-33.

Giamarellou H, Kanellakopoulou K (2008) Current therapies for pseudomonas aeruginosa. Crit Care Clin 24(2): 261-78, viii.

Giamarellou H, Zissis NP, Tagari G, Bouzos J (1984) In vitro synergistic activities of aminoglycosides and new beta-lactams against multiresistant Pseudomonas aeruginosa. Antimicrob Agents Chemother 25(4): 534-6.

Gristina AG, Shibata Y, Giridhar G, Kreger A, Myrvik QN (1994) The glycocalyx, biofilm, microbes, and resistant infection. Semin Arthroplasty 5(4): 160-70.

Haley RW, Bregman DA (1982) The role of understaffing and overcrowding in recurrent outbreaks of staphylococcal infection in a neonatal special-care unit. J Infect Dis 145(6): 875-85.

Hanberger H, Diekema D, Fluit A, Jones R, Struelens M, Spencer R, Wolff M (2001) Surveillance of antibiotic resistance in European ICUs. J Hosp Infect 48(3): 161-76.

Hancock RE (1998) Resistance mechanisms in Pseudomonas aeruginosa and other nonfermentative gram-negative bacteria. Clin Infect Dis 27 Suppl 1: S93-9.

Harder ME, Ladenson RC, Schimmel SD, Silbert DF (1974) Mutants of Escherichia coli with temperature-sensitive malonyl coenzyme A-acyl carrier protein transacylase. J Biol Chem 249(23): 7468-75.

Harris AA, Goodman L, Levin S (1984) Community-acquired Pseudomonas aeruginosa pneumonia associated with the use of a home humidifier. West J Med 141(4): 521-3.

Hayashi T, Yamamoto O, Sasaki H, Okazaki H, Kawaguchi A (1984) Inhibition of fatty acid synthesis by the antibiotic thiolactomycin. J Antibiot (Tokyo) 37(11): 1456-61.

Heath RJ, Rock CO (1996) Roles of the FabA and FabZ beta-hydroxyacyl-acyl carrier protein dehydratases in Escherichia coli fatty acid biosynthesis. J Biol Chem 271(44): 27795-801.

Heath RJ, Rock CO (2004) Fatty acid biosynthesis as a target for novel antibacterials. Curr Opin Investig Drugs 5(2): 146-53.

Heath RJ, White SW, Rock CO (2001) Lipid biosynthesis as a target for antibacterial agents. Prog Lipid Res 40(6): 467-97.

Heath RJ, Yu YT, Shapiro MA, Olson E, Rock CO (1998) Broad spectrum antimicrobial biocides target the FabI component of fatty acid synthesis. J Biol Chem 273(46): 30316-20.

Helmkamp GM Jr., Bloch K (1969) Beta-hydroxydecanoyl thioester dehydrase. Studies on molecular structure and active site. J Biol Chem 244(21): 6014-22.

Hoang TT, Schweizer HP (1997) Fatty acid biosynthesis in Pseudomonas aeruginosa: cloning and characterization of the fabAB operon encoding beta-hydroxyacyl-acyl carrier protein dehydratase (FabA) and beta-ketoacyl-acyl carrier protein synthase I (FabB). J Bacteriol 179(17): 5326-32.

Hogan D, Kolter R (2002) Why are bacteria refractory to antimicrobials? Curr Opin Microbiol 5(5): 472-7.

Hoiby N (1993) Cystic fibrosis and endobronchial pseudomonas infection. Curr Opin Pediatr 5(3): 247-54.

Hoiby N, Krogh Johansen H, Moser C, Song Z, Ciofu O, Kharazmi A (2001) Pseudomonas aeruginosa and the in vitro and in vivo biofilm mode of growth. Microbes Infect 3(1): 23-35.

Holland SP, Pulido JS, Shires TK, Costerton JW (1993) Pseudomonas aeruginosaocular infections. In: Pseudomonas aeruginosa. Fick RB Jr, (ed.) The Opportunist. Boca Raton: CRC Press 159-176.

Honeyman G, Fawcett T (2000) Protein interactions of fatty acid synthase II. Biochem Soc Trans 28(6): 615-6.

Huang W, Jia J, Edwards P, Dehesh K, Schneider G, Lindqvist Y (1998) Crystal structure of beta-ketoacyl-acyl carrier protein synthase II from E.coli reveals the molecular architecture of condensing enzymes. EMBO J 17(5): 1183-91.

Jackowski S, Rock CO (1987) Acetoacetyl-acyl carrier protein synthase, a potential regulator of fatty acid biosynthesis in bacteria. J Biol Chem 262(16): 7927-31.

Jo JT, Brinkman FS, Hancock RE (2003) Aminoglycoside efflux in Pseudomonas aeruginosa: involvement of novel outer membrane proteins. Antimicrob Agents Chemother 47(3): 1101-11.

Jones RN, Kirby JT, Beach ML, Biedenbach DJ, Pfaller MA (2002) Geographic variations in activity of broad-spectrum beta-lactams against Pseudomonas aeruginosa: summary of the worldwide SENTRY Antimicrobial Surveillance Program (1997-2000). Diagn Microbiol Infect Dis 43(3): 239-43.

Jones SM, Urch JE, Brun R, Harwood JL, Berry C, Gilbert IH (2004) Analogues of thiolactomycin as potential anti-malarial and anti-trypanosomal agents. Bioorg Med Chem 12(4): 683-92.

Kabsch W Xds. Acta Crystallogr D Biol Crystallogr 66(Pt 2): 125-32.

Kardos N, Demain AL (2011) Penicillin: the medicine with the greatest impact on therapeutic outcomes. Appl Microbiol Biotechnol. 92(4):677-87.

Karlowsky JA, Draghi DC, Jones ME, Thornsberry C, Friedland IR, Sahm DF (2003) Surveillance for antimicrobial susceptibility among clinical isolates of Pseudomonas aeruginosa and Acinetobacter baumannii from hospitalized patients in the United States, 1998 to 2001. Antimicrob Agents Chemother 47(5): 1681-8.

Kass LR, Bloch K (1967) On the enzymatic synthesis of unsaturated fatty acids in Escherichia coli. Proc Natl Acad Sci 58(3): 1168–1173.

Kauppinen S, Siggaard-Andersen M, von Wettstein-Knowles P (1988) beta-Ketoacyl-ACP synthase I of Escherichia coli: nucleotide sequence of the fabB gene and identification of the cerulenin binding residue. Carlsberg Res Commun 53(6): 357-70.

Khandekar SS, Gentry DR, Van Aller GS, Warren P, Xiang H, Silverman C, Doyle ML, Chambers PA, Konstantinidis AK, Brandt M, Daines RA, Lonsdale JT (2001) Identification, substrate specificity, and inhibition of the Streptococcus pneumoniae beta-ketoacyl-acyl carrier protein synthase III (FabH). J Biol Chem 276(32): 30024-30.

Kharami A, Bibi Z, Nielsen H, Hoiby N, Döring G (1989) Effect of Pseudomonas aeruginosa rhamnolipid on human neutrophil and monocyte function. APMIS 97(12): 1068-72.

Kimber MS, Martin F, Lu Y, Houston S, Vedadi M, Dharamsi A, Fiebig KM, Schmid M, Rock CO (2004) The structure of (3R)-hydroxyacyl-acyl carrier protein dehydratase (FabZ) from Pseudomonas aeruginosa. J Biol Chem 279(50): 52593-602.

Kiska DL, Gilligan PH (2003) Pseudomonas. In: Manual of Clinical Microbiology.Murray PR, Baron EJ, Jorgensen JH, Pfaller MH, Yolken RH(eds.) 8th edn. Washington. ASM Press 719-728.

Klebe G (2000) Recent developments in structure-based drug design. J Mol Med 78(5): 269-81.

Klemm P, Hancock V, Kvist M, Schembri MA (2007) Candidate targets for new antivirulence drugs: selected cases of bacterial adhesion and biofilm formation. Future Microbiol 2(6): 643-53.

Klevens RM, Edwards JR, Richards CL Jr, Horan TC, Gaynes RP, Pollock DA, Cardo DM (2007) Estimating health care-associated infections and deaths in U.S. hospitals, 2002. Public Health Rep 122(2):160-6.

Kohler T, Michea-Hamzehpour M, Henze U, Gotoh N, Curty LK, Pechere JC (1997) Characterization of MexE-MexF-OprN, a positively regulated multidrug efflux system of Pseudomonas aeruginosa. Mol Microbiol 23(2): 345-54.

Kohler T, Pechere C (2001) In vitro selection of antibiotic resistance in Pseudomonas aeruginosa. Clin Microbiol Infect 7 Suppl 5: 7-10.

Koll BS, Brown AE (1993) The changing epidemiology of infections at cancer hospitals. Clin Infect Dis 17 Suppl 2: S322-8.

Kollef MH, Fraser VJ (2001) Antibiotic resistance in the intensive care unit. Ann Intern Med 134(4): 298-314.

Kollef MH, Micek ST (2005) Strategies to prevent antimicrobial resistance in the intensive care unit. Crit Care Med 33(8): 1845-53.

Komori Y, Nonogaki T, Nikai T (2001) Hemorrhagic activity and muscle damaging effect of Pseudomonas aeruginosa metalloproteinase (elastase). Toxicon 39(9): 1327-32.

Lange RP, Locher HH, Wyss PC, Then RL (2007) The targets of currently used antibacterial agents: lessons for drug discovery. Curr Pharm Des 13(30): 3140-54.

Leesong M, Henderson BS, Gillig JR, Schwab JM, Smith JL (1996) Structure of a dehydratase-isomerase from the bacterial pathway for biosynthesis of unsaturated fatty acids: two catalytic activities in one active site. Structure 4(3): 253-64.

Lehninger AL, Nelson DL, Cox MM (1998) Prinzipien der Biochemie. 2. Aufl., Spektrum Akademischer Verlag, Heidelberg.

Levy CW, Roujeinikova A, Sedelnikova S, Baker PJ, Stuitje AR, Slabas AR, Rice DW, Rafferty JB (1999) Molecular basis of triclosan activity." Nature 398(6726): 383-4.

Lewenza S, Gardy JL, Brinkman FS, Hancock RE (2005) Genome-wide identification of Pseudomonas aeruginosa exported proteins using a consensus computational strategy combined with a laboratory-based PhoA fusion screen. Genome Res 15(2): 321-9.

Lister PD, Wolter DJ, Hanson ND (2009) Antibacterial-resistant Pseudomonas aeruginosa: clinical impact and complex regulation of chromosomally encoded resistance mechanisms. Clin Microbiol Rev. 22(4):582-610.

Liu H, Naismith JH (2008) An efficient one-step site-directed deletion, insertion, single and multiple-site plasmid mutagenesis protocol. BMC Biotechnol 8: 91.

Liu W, Han C, Hu L, Chen K, Shen X, Jiang H (2006) Characterization and inhibitor discovery of one novel malonyl-CoA: acyl carrier protein transacylase (MCAT) from Helicobacter pylori. FEBS Lett 580(2): 697-702.

Livermore DM (1992) Interplay of impermeability and chromosomal beta-lactamase activity in imipenem-resistant Pseudomonas aeruginosa. Antimicrob Agents Chemother 36(9): 2046-8.

Livermore DM (1995) beta-Lactamases in laboratory and clinical resistance. Clin Microbiol Rev 8(4): 557-84.

Livermore DM (2001) Of Pseudomonas, porins, pumps and carbapenems. J Antimicrob Chemother 47(3): 247-50.

Lu YJ, White SW, Rock CO (2005) Domain swapping between Enterococcus faecalis FabN and FabZ proteins localizes the structural determinants for isomerase activity. J Biol Chem 280(34): 30342-8.

Lutz F, Xiong G, Jungblut R, Orlik-Eisel G, Göbel-Reifert A, Leidorf R (1991) Pore-forming cytotoxin of Pseudomonas aeruginosa: the molecular effects and aspects of pathogenicity. Antibiot Chemother 44: 54-8.

Magnuson K, Jackowski S, Rock CO, Cronan JE Jr. (1993) Regulation of fatty acid biosynthesis in Escherichia coli. Microbiol Rev 57(3): 522-42.

Mahoney JF, Arnold RC, Harris A (1943) Penicillin Treatment of Early Syphilis-A Preliminary Report. Am J Public Health Nations Health 33(12): 1387-91.

Marrakchi H, Dewolf WE Jr., Quinn C, West J, Polizzi BJ, So CY, Holmes DJ, Reed SL, Heath RJ, Payne DJ, Rock CO, Wallis NG (2003) Characterization of Streptococcus pneumoniae enoyl-(acyl-carrier protein) reductase (FabK). Biochem J 370(Pt 3): 1055-62.

Martone WJ, Jarvis WR, Culver DH, Haley RW (1992) Incidence and nature of endemic and epidemic nosocomial infections. In: Hospital infections.Bennett JV, Brachman PS (eds.), Little, Brown and Company, Boston 577-96.

Mayhall CG (1997) Nosocomial pneumonia. Diagnosis and prevention. Infect Dis Clin North Am 11(2): 427-57.

McCoy AJ, Grosse-Kunstleve RW, Adams PD, Winn MD, Storoni LC, Read RJ (2007) Phaser crystallographic software. J Appl Crystallogr 40(Pt 4): 658-674.

McGowan JE Jr. (2006) Resistance in nonfermenting gram-negative bacteria: multidrug resistance to the maximum. Am J Infect Control 34(5 Suppl 1): S29-37; discussion S64-73.

McMurry LM, Oethinger M, Levy SB (1998) Triclosan targets lipid synthesis. Nature 394(6693): 531-2.

Miyakawa S, Suzuki K, Noto T, Harada Y, Okazaki H (1982) Thiolactomycin, a new antibiotic. IV. Biological properties and chemotherapeutic activity in mice. J Antibiot (Tokyo) 35(4): 411-9.

Mohan S, Kelly TM, Eveland SS, Raetz CR, Anderson MS (1994) An Escherichia coli gene (FabZ) encoding (3R)-hydroxymyristoyl acyl carrier protein dehydrase. Relation to fabA and suppression of mutations in lipid A biosynthesis. J Biol Chem 269(52): 32896-903.

Morrison AJ Jr., Wenzel RP (1984) Epidemiology of infections due to Pseudomonas aeruginosa. Rev Infect Dis 6 Suppl 3: S627-42.

Mousa HA (1997) Aerobic, anaerobic and fungal burn wound infections. J Hosp Infect 37(4): 317-23.

Moynié L, Leckie SM, McMahon SA, Duthie FG, Koehnke A, Taylor JW, Alphey MS, Brenk R, Smith AD, Naismith JH. (2013) Structural insights into the mechanism and inhibition of the β-hydroxydecanoyl-acyl carrier protein dehydratase from Pseudomonas aeruginosa. J Mol Biol. 425(2):365-77.

Murray TS, Egan M, Kazmierczak BI (2007) Pseudomonas aeruginosa chronic colonization in cystic fibrosis patients. Curr Opin Pediatr 19(1): 83-8.

National Nosocomial Infections Surveillance (NNIS) System Report: data summary from October 1986 to April 1998, issued June1998. Am J Infect Control 1988; 26: 522-533.

Nicas TI, Bradley J, Lochner JE, Iglewski BH (1985) The role of exoenzyme S in infections with Pseudomonas aeruginosa. J Infect Dis 152(4): 716-21.

Nikolskaya T, Zagnitko O, Tevzadze G, Haselkorn R, Gornicki P (1999) Herbicide sensitivity determinant of wheat plastid acetyl-CoA carboxylase is located in a 400-amino acid fragment of the carboxyltransferase domain. Proc Natl Acad Sci U S A 96(25):14647-51.

Normark BH, Normark S (2002) Evolution and spread of antibiotic resistance. J Intern Med 252(2): 91-106.

Noto T, Miyakawa S, Oishi H, Endo H, Okazaki H (1982) Thiolactomycin, a new antibiotic. III. In vitro antibacterial activity. J Antibiot (Tokyo) 35(4): 401-10.

Perron GG, Kryazhimskiy S, Rice DP, Buckling A (2012) Multidrug-therapy and evolution of antibiotic resistance: When order matters. Appl Environ Microbiol.

Piddock LJ (1999) Mechanisms of fluoroquinolone resistance: an update 1994-1998. Drugs 58 Suppl 2: 11-8.

Pittet D, Allegranzi B, Sax H, Dharan S, Pessoa-Silva CL, Donaldson L, Boyce JM (2006) Evidence-based model for hand transmission during patient care and the role of improved practices. Lancet Infect Dis 6(10): 641-52.

Pizzo PA (1999) Fever in immunocompromised patients. N Engl J Med 341(12): 893-900.

Pollack M (1980) Pseudomonas aeruginosa exotoxin A. N Engl J Med 302(24): 1360-2.

Pollack M (2000) Pseudomonas aeruginosa. In: Principles and Practice of Infectious Diseases. Mandell GL, Bennett JE, Dolin R (eds.),5th edn. Philadelphia, Churchill Livingstone, 2000: 2310–2335.

.

Poole K (2001) Multidrug efflux pumps and antimicrobial resistance in Pseudomonas aeruginosa and related organisms. J Mol Microbiol Biotechnol 3(2): 255-64.

Poole K (2002) Mechanisms of bacterial biocide and antibiotic resistance. J Appl Microbiol 92 Suppl: 55S-64S.

Poole K (2004) Efflux-mediated multiresistance in Gram-negative bacteria. Clin Microbiol Infect 10(1): 12-26.

Poole K (2005) Aminoglycoside resistance in Pseudomonas aeruginosa. Antimicrob Agents Chemother 49(2): 479-87.

Poole K, Srikumar R(2001) Assessing the activity of bacterial multidrug efflux pumps. Methods Mol Med 48: 211-4.

Poulakou G, Giamarellou H (2008) Doripenem: an expected arrival in the treatment of infections caused by multidrug-resistant Gram-negative pathogens. Expert Opin Investig Drugs 17(5): 749-71.

Price AC, Rock CO, White SW (2003) The 1.3-Angstrom-resolution crystal structure of beta-ketoacyl-acyl carrier protein synthase II from Streptococcus pneumoniae. J Bacteriol 185(14): 4136-43.

Price AC, Zhang YM, Rock CO, White SW (2001) Structure of beta-ketoacyl-[acyl carrier protein] reductase from Escherichia coli: negative cooperativity and its structural basis. Biochemistry 40(43): 12772-81.

Prince A (1992) Adhesins and receptors of Pseudomonas aeruginosa associated with infection of the respiratory tract. Microb Pathog 13(4): 251-60.

Rahal JJ (2008) The role of carbapenems in initial therapy for serious Gram-negative infections. Crit Care 12 Suppl 4: S5.

Rajashekaraiah KR, Rice TW, Kallick CA (1981) Recovery of Pseudomonas aeruginosa from syringes of drug addicts with endocarditis. J Infect Dis 144(5): 482.

Ramphal R, Pier GB (1985) Role of Pseudomonas aeruginosa mucoid exopolysaccharide in adherence to tracheal cells. Infect Immun 47(1): 1-4.

Rampling A, Wiseman S, Davis L, Hyett AP, Walbridge AN, Payne GC, Cornaby AJ (2001) Evidence that hospital hygiene is important in the control of methicillin-resistant Staphylococcus aureus. J Hosp Infect 49(2): 109-16.

Read RC, Roberts P, Munro N, Rutman A, Hastie A, Shryock T, Hall R, McDonald-Gibson W, Lund V, Taylor G (1992) Effect of Pseudomonas aeruginosa rhamnolipids on mucociliary transport and ciliary beating. J Appl Physiol 72(6): 2271-7.

Reinhardt A, Kohler T, Wood P, Rohner P, Dumas JL, Ricou B, van Delden C (2007) Development and persistence of antimicrobial resistance in Pseudomonas aeruginosa: a longitudinal observation in mechanically ventilated patients. Antimicrob Agents Chemother 51(4): 1341-50.

Rieder HL, Cauthen GM, Kelly GD, Bloch AB, Snieder DE Jr. (1989) Tuberculosis in the United States. JAMA 262(3): 385-9.

Rock CO, Cronan JE(1996) Escherichia coli as a model for the regulation of dissociable (type II) fatty acid biosynthesis. Biochim Biophys Acta 1302(1): 1-16.

Rosenfeld IS, D'Agnolo G, Vagelos PR (1973) Synthesis of unsaturated fatty acids and the lesion in fab B mutants. J Biol Chem 248(7): 2452-60.

Rossolini GM, Mantengoli E (2005) Treatment and control of severe infections caused by multiresistant Pseudomonas aeruginosa. Clin Microbiol Infect 11 Suppl 4: 17-32.

Rubin J, Yu VL (1988) Malignant external otitis: insights into pathogenesis, clinical manifestations, diagnosis, and therapy. Am J Med 85(3): 391-8.

Sandiumenge A, Diaz E, Rodriguez A, Vidaur L, Canadell L, Olona M, Rue M, Rello J (2006) Impact of diversity of antibiotic use on the development of antimicrobial resistance. J Antimicrob Chemother 57(6): 1197-204.

Schwab JM, Klassen JB, Lin DC (1985) beta-Hydroxydecanoylthioester dehydrase: a rapid, convenient, and accurate product distribution assay. Anal Biochem 150(1): 121-4.

Sharma SK, Kapoor M, Ramya TN, Kumar S, Kumar G, Modak R, Sharma S, Surolia N, Surolia A (2003) Identification, characterization, and inhibition of Plasmodium falciparum beta-hydroxyacyl-acyl carrier protein dehydratase (FabZ). J Biol Chem 278(46): 45661-71.

Silbert DF, Vagelos PR (1967) Fatty acid mutant of E. coli lacking a beta-hydroxydecanoyl thioester dehydrase. Proc Natl Acad Sci U S A 58(4): 1579-86.

Slayden RA, Lee RE, Armour JW, Cooper AM, Orme IM, Brennan PJ, Besra GS (1996) Antimycobacterial action of thiolactomycin: an inhibitor of fatty acid and mycolic acid synthesis. Antimicrob Agents Chemother 40(12): 2813-9.

Spellberg B, Powers JH, Brass EP, Miller LG, Edwards JE Jr. (2004) Trends in antimicrobial drug development: implications for the future. Clin Infect Dis 38(9): 1279-86.

Spencer RC (1996) Predominant pathogens found in the European Prevalence of Infection in Intensive Care Study. Eur J Clin Microbiol Infect Dis 15(4): 281-5.

Stewart PS, Rayner J, Roe F, Rees WM (2001) Biofilm penetration and disinfection efficacy of alkaline hypochlorite and chlorosulfamates. J Appl Microbiol 91(3): 525-32.

Stover CK, Pham XQ, Erwin AL, Mizoguchi SD, Warrener P, Hickey MJ, Brinkman FS, Hufnagle WO, Kowalik DJ, Lagrou M, Garber RL, Goltry L. Tolentino E, Westbrock-Wadman S, Yuan Y, Brody LL, Coulter SN, Folger KR, Kas A, Larbig K, Lim R, Smith K, Spencer D, Wong GK, Wu Z, Paulsen IT, Reizer J, Saier MH, Hancock RE, Lory S, Olsen MV (2000) Complete genome sequence of Pseudomonas aeruginosa PAO1, an opportunistic pathogen. Nature 406(6799): 959-64.

Thomson JM, Bonomo RA (2005) The threat of antibiotic resistance in Gram-negative pathogenic bacteria: beta-lactams in peril! Curr Opin Microbiol 8(5): 518-24.

Tsay JT, Oh W, Larson TJ, Jackowski S, Rock CO (1992) Isolation and characterization of the beta-ketoacyl-acyl carrier protein synthase III gene (fabH) from Escherichia coli K-12. J Biol Chem 267(10): 6807-14.

Van Delden C, Iglewski BH (1998) Cell-to-cell signaling and Pseudomonas aeruginosa infections. Emerg Infect Dis 4(4): 551-60.

Wacha H (1999) Infektiologie heute- Zeit zum Umdenken, München, W. Zuckschwerdt Verlag, XI-XIV.

Walsh C, Wright G (2005) Introduction: antibiotic resistance. Chem Rev 105(2): 391-4.

Walsh TR, Toleman MA, Poirel L, Nordmann P (2005) Metallo-beta-lactamases: the quiet before the storm? Clin Microbiol Rev 18(2): 306-25.

Wang J, Kodali S, Lee SH, Galgoci A, Painter R, Dorso K, Racine F, Motyl M, Hernandez L, Tinney E, Colletti SL, Herath K, Cummings R, Salazar O, Gonzales I, Basilio A, Vicente F, Genilloud O, Pelaez F, Jayasuriya H, Young K, Cully DF, Singh SB (2007) Discovery of platencin, a dual FabF and FabH inhibitor with in vivo antibiotic properties. Proc Natl Acad Sci U S A 104(18): 7612-6.

Wang J, Soisson SM, Young K, Shoop W, Kodali S, Galgoci A, Painter R, Parthasarathy G, Tang YS, Cummings R, Ha S, Dorso K, Motyl M, Jayasuriya H, Ondeyka J, Herath K, Zhang C, Hernandez L, Allocco J, Basilio A, Tormo JR, Genilloud O, Vicente F, Pelaez F, Colwell L, Lee SH, Michael B, Felcetto T, Gill C, Silver LL, Hermes JD, Bartizal K, Barrett J, Schmatz D, Becker JW, Cully D, Singh SB (2006) Platensimycin is a selective FabF inhibitor with potent antibiotic properties. Nature 441(7091): 358-61.

Warren DK, Hill HA, Merz LR, Kollef MH, Hayden MK, Fraser VJ, Fridkin SK (2004) Cycling empirical antimicrobial agents to prevent emergence of antimicrobial-resistant Gram-negative bacteria among intensive care unit patients. Crit Care Med 32(12): 2450-6.

Weldhagen GF, Poirel L, Nordmann P (2003) Ambler class A extended-spectrum beta-lactamases in Pseudomonas aeruginosa: novel developments and clinical impact. Antimicrob Agents Chemother 47(8): 2385-92.

Welsh MJ, Smith AE (1995) Cystic fibrosis. Sci Am 273(6): 52-9.

White DG, McDermott PF (2001) Biocides, drug resistance and microbial evolution. Curr Opin Microbiol 4(3): 313-7.

White SW, Zheng J, Zhang YM, Rock (2005) The structural biology of type II fatty acid biosynthesis. Annu Rev Biochem 74: 791-831.

Wimpenny J, Manz W, Szewzyk U (2000) Heterogeneity in biofilms. FEMS Microbiol Rev 24(5): 661-71.

Yuan Z, Tam VH (2008) Polymyxin B: a new strategy for multidrug-resistant Gram-negative organisms. Expert Opin Investig Drugs 17(5): 661-8.

Zhang YM, Rock CO (2004) Evaluation of epigallocatechin gallate and related plant polyphenols as inhibitors of the FabG and FabI reductases of bacterial type II fatty-acid synthase. J Biol Chem 279(30): 30994-1001.

7 ACKNOWLEDGEMENT

I would like to specially thank my tutor, Prof. Friedrich, for taking me on as a student and making my stay in St Andrews possible. His many helpful comments with regards to my writing greatly enhanced the final result.

I would like to thank Prof. Naismith for allowing me to work in his laboratory and his critical reading of my thesis.

I would like to thank Dr. Lucile Moynie her patience and expert guidance as well as her helpful comments during the writing of this thesis.

I would like to thank Mr. Fraser Duthie for the excellent support as well as the friendly welcome to the working group, where I felt most comfortable.

Finally I would like to thank my parents and my brother Jesko Köhnke. Without your support this work would have been much more difficult.

8 CURRICULUM VITAE

Entfällt aus datenschutzrechtlichen Gründen

9 AFFIDAVIT

Ich versichere ausdrücklich, dass ich die Arbeit selbständig und ohne fremde Hilfe verfasst, andere als die von mir angegebenen Quellen und Hilfsmittel nicht benutzt und die aus den benutzten Werken wörtlich oder inhaltlich entnommenen Stellen einzeln nach Ausgabe (Auflage und Jahr des Erscheinens), Band und Seite des benutzten Werkes kenntlich gemacht habe.

Ferner versichere ich, dass ich die Dissertation bisher nicht einem Fachvertreter an einer anderen Hochschule zur Überprüfung vorgelegt oder mich anderweitig um Zulassung zur Promotion beworben habe.

Unterschrift: .....

APPENDIX

Hydrogen bonds

	Structure 1	Dist. [Å]	Structure 2
1	F:ALA 30[N]	2.85	E:CYS 69[O]
2	F:GLN 27[NE2]	2.81	E:GLU 72[O]
3	F:ARG 104[NH2]	2.85	E:ASP 74[OD1]
4	F:ARG 104[NH1]	2.78	E:ASP 74[OD2]
5	F:PHE 113[N]	2.88	E:LEU 106[O]
6	F:VAL 111[N]	2.87	E:SER 108[O]
7	F:SER 108[N]	2.89	E:VAL 111[O]
8	F:ARG 104[NE]	2.94	E:GLN 116[OE1]
9	F:ARG 104[NH2]	3.13	E:GLN 116[OE1]
10	F:GLN 116[N]	3.81	E:PHE 171[OXT]
11	F:CYS 69[O]	2.79	E:ALA 30[N]
12	F:GLU 72[O]	2.82	E:GLN 27[NE2]
13	F:ASP 74[OD1]	3.09	E:ARG 104[NH2]
14	F:ASP 74[OD2]	3.05	E:ARG 104[NH1]
15	F:LEU 106[O]	2.86	E:PHE 113[N]
16	F:SER 108[O]	2.83	E:VAL 111[N]
17	F:VAL 111[O]	2.97	E:SER 108[N]
18	F:GLN 116[OE1]	3.15	E:ARG 104[NH2]
19	F:GLN 116[OE1]	3.00	E:ARG 104[NE]
20	F:PHE 171[OXT]	3.31	E:ARG 152[NH2]

Salt bridges

	Structure 1	Dist. [Å]	Structure 2
1	F:ARG 104[NH2]	2.85	E:ASP 74[OD1]
2	F:ARG 102[NE]	3.83	E:ASP 74[OD1]
3	F:ARG 104[NH1]	3.80	E:ASP 74[OD1]
4	F:ARG 104[NH2]	3.39	E:ASP 74[OD2]
5	F:ARG 102[NE]	3.83	E:ASP 74[OD2]
6	F:ARG 104[NH1]	2.78	E:ASP 74[OD2]
7	F:ASP 74[OD1]	3.09	E:ARG 104[NH2]
8	F:ASP 74[OD2]	3.67	E:ARG 102[NE]
9	F:ASP 74[OD2]	3.05	E:ARG 104[NH1]
10	F:ASP 74[OD2]	3.48	E:ARG 104[NH2]